Received: 4 April 2022 | Revised: 13 December 2022 | Accepted: 10 March 2023

DOI: 10.1002/dvdy.589

Developmental Dynamics WILEY

REVIEW

Experimental assessment of cardiovascular physiology in the chick embryo

Vijayakumar Sukumaran[1] | Onur Mutlu[1] | Mohammad Murtaza[1] | Rawia Alhalbouni[1] | Benjamin Dubansky[2] | Huseyin C. Yalcin[1,3]

[1]Biomedical Research Center, Qatar University, Doha, Qatar

[2]Department of Biological and Agricultural Engineering, Office of Research and Economic Development, Louisiana State University, Baton Rouge, Louisiana, USA

[3]Department of Biomedical Science, College of Health Sciences, QU Health, Qatar University, Doha, Qatar

Correspondence
Huseyin C. Yalcin, Biomedical Research Center, Qatar University, Doha, Qatar.
Email: hyalcin@qu.edu.qa

Funding information
Qatar National Library; Qatar National Research Fund, Grant/Award Number: NPRP 10-0123-170222

Abstract

High resolution assessment of cardiac functional parameters is crucial in translational animal research. The chick embryo is a historically well-used in vivo model for cardiovascular research due to its many practical advantages, and the conserved form and function of the chick and human cardiogenesis programs. This review aims to provide an overview of several different technical approaches for chick embryo cardiac assessment. Doppler echocardiography, optical coherence tomography, micromagnetic resonance imaging, microparticle image velocimetry, real-time pressure monitoring, and associated issues with the techniques will be discussed. Alongside this discussion, we also highlight recent advances in cardiac function measurements in chick embryos.

KEYWORDS

blood flow, blood flow velocity, cardiac function, cardiac physiology, chick embryo, Doppler, echocardiography, hemodynamics, magnetic resonance imaging, optical coherence tomography, pressure, shear stress

1 | INTRODUCTION

Cardiovascular disease is the major cause of mortality worldwide, accounting for 17.3 million annual deaths, predicted to increase to 23.6 million by 2030.[1] Not surprisingly, congenital heart defects (CHDs) are the most common of birth defects.[2] Numerous inherent and environmental factors interact to manage and affect the cardiac developmental program. However, as soon as blood begins to move through the heart and vasculature, hemodynamic forces begin to play a major role in initiating and enhancing signaling pathways that drive cardiac morphogenesis, angiogenesis, and the cardiac conduction system development.[3-6] Consequently, alteration of hemodynamics during development significantly alters the developmental trajectory of the cardiovascular system through chronic cardiovascular impairment in vertebrates.[7-9] Indeed, disturbed hemodynamics during the embryo stages are a major factor contributing to the development of CHDs in humans.[10,11]

Due to difficulties in accessing the human fetus, animal studies are instrumental in studying how hemodynamics contribute to the patterning of the developing heart. The chick embryo (*Gallus gallus domesticus*) is a particularly well-established model organism for developmental physiology research for over 2000 years, with roots going back to Aristotle.[12,13] The popularity of the chick embryo as a cardiovascular model arose mainly due to the visibility and accessibility of the heart and vasculature during early development, when the embryo

resides on top of the yolk as it develops into a chick hatchling. Thus, the chick embryo's heart and vasculature are visible and accessible for experimentation by removing a small piece of eggshell (Figure 1). Due to these attributes and the accessibility of chicken eggs, it is not surprising that the chick embryo has become established as a premier developmental animal model for studying cardiovascular physiology[14] and an excellent platform to explore the influences of hemodynamic forces within the cardiovascular system.[15-17]

The chick embryo model is also helpful in studying new blood vessel formation (angiogenesis/vasculogenesis).[18] The intraembryonic and extraembryonic vitelline vessels branch across the yolk in a predictable pattern. Commonly referred to as the chorioallantoic membrane (CAM) vasculature, arteries, and veins are easily accessible since they are distributed over the top of the yolk (Figure 1). CAM vasculature is a well-established model for study of angiogenesis/vasculogenesis, where variables in the development of vascular patterns during embryonic development can be conveniently monitored.[19] For qualitative and quantitative assessment of angiogenesis in the chick embryo CAM model, blood flow in these models need to be examined by measuring flow velocity and pressure, which would then be used to calculate hemodynamic forces.

Hemodynamic forces have a powerful influence over angiogenesis, where forces from pressure and flow drive the process of new vessel formation and healthy patterning of new vasculature; such that abnormal hemodynamics can cause altered vascular formation which can alter the functional efficacy of otherwise healthy tissue.[20] Indeed, altered blood flow patterns during development are often associated with CHDs.[6,21-27] Unfortunately, the vascular network is complex, with increasing variation in the branching pattern with increased distance from the great vessels and time of development. Thus, the well-characterized patterns of healthy vascular development in chicken embryos provides a platform for understanding how changes in hemodynamics affect vascular branching pattern and function. Over the many years since Aristotle's Day, different techniques have been adapted and scaled down to measure the tiny, yet scalable hemodynamic forces in chick embryos as a model for cardiovascular developmental physiology. Through these physiological tools, we can build clinically relevant cardiac defects while evaluating the physiological relevance between animal and human models. Though not a comprehensive review of the many tools that we have seen, this short review highlights some techniques that enabled us to assess the development of hemodynamic forces in the chick embryo.

In recent decades, technologies have allowed techniques from human clinics to be applied to the chick embryology. Doppler echocardiography, optical coherence tomography (OCT) and μ-MRI systems allow diagnostic medical imaging to detect blood flow and assess tissue structure in these tiny embryos. In addition, digital image analysis tools are commonly applied alongside microscopy to characterize blood flow in even capillary-sized vessels. Flow sensing is largely based on imaging technologies. High-resolution techniques, including Doppler echocardiography and 3D-OCT, could prove considerable importance, particularly for the real-time assessment of cardiac functional parameters. These techniques have proven successful in screening for vascular defects,[28] and monitoring cardiac flow velocities.[29] Doppler echocardiography is a unique technique that is widely used for accessing hemodynamic alteration.[30] Compared to traditional ultrasound, OCT has a superior resolution (5–10 μm) and is thus better suited for imaging smaller structures (eg, embryonic hearts and vasculature). However, OCT's longer operating wavelengths limit the penetration depth to nearly 2 mm. Hence, it is not practical

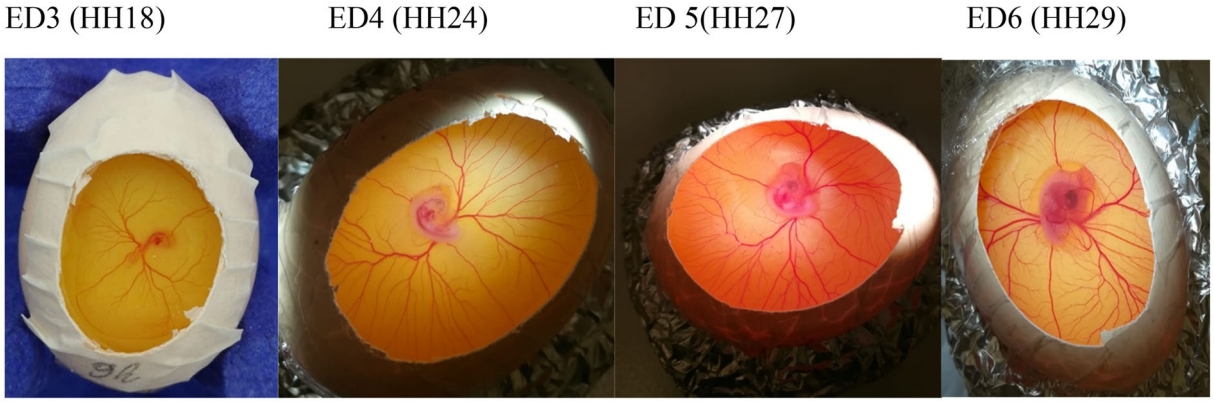

FIGURE 1 Pictures of chick embryos, stage HH18 to HH29 (embryonic days 3–6) cultured in-ovo. ED, embryonic development; HH, Hamburger & Hamilton.

for deep tissue imaging, but OCT is quite valid for the accessible vasculature of embryonic chicks.[31-34] Using OCT imaging of blood flow, blood velocity and shear stress levels in the endocardium have been established in various animal models, including Drosophila,[35] chick embryo,[36] mouse,[37] and xemopus laevis.[38]

Transducers in pressure sensing in microenvironments have also enabled techniques to be scaled for smaller applications built around increasingly sensitive optical and electrophysiological pressure transducers. However, it is difficult to assess blood pressure (BP) in embryos due to the necessity for accessing the inside of the cardiovascular system and the targeted structure's small size. Several techniques can be applied to chick embryos to assess pressure within cardiovascular compartments in the vasculature and heart. Complex pressure waveforms within the heart or blood vessels can be measured directly via catheters connected to pressure transducers,[39,40] or by the servo-null micropressure technique, which employs a unique transduction system to monitor subtle changes in pressure by sensing changes in the electrochemical properties of an electrolyte-filled glass capillary.[41] Such electrophysiological techniques have been used to study pressure in chick embryos,[42] zebrafish hearts,[43] and cells.[44]

This review summarizes the most common in vivo techniques applied to chick embryos for assessing cardiac functional parameters. We discuss how these methodologies have been used for both improved visualization of embryonic development and to enable precise measurement of blood flow and pressure in the cardiovascular system of the embryonic chick. As we present these techniques, we provide contextual data to illustrate how pressure and flow velocities change during development in the chick embryo.

1.1 | Measurement of blood flow velocity (BFV)

Understanding cardiovascular flow characteristics is essential to study cardiac functions and the progression of disease. Several technologies to monitor flow velocities through blood vessels and cardiac chambers in human clinic and in mammalian model organisms are adapted for use in chicken embryos.[29,45,46] Common targets for analysis of BFV are the vitelline vessels, atrioventricular (AV) canal and outflow tract (OFT). These targets are readily accessible, and investigations commonly involve interference of CAM, AV canal, and OFT to investigate effects of altered hemodynamics within the developing cardiovascular system. Importantly, there are macroscopic and microscopic techniques for the study of BFV. Utilized measurement techniques include Doppler ultrasound, Doppler OCT, and microresolution particle image velocimetry (μ-PIV). In addition, μ-MRI technologies have been recently applied to measure blood flow.

1.2 | Doppler echocardiography

Echocardiography is a widely used noninvasive type of medical imaging modality of the heart that relies on ultrasound technology to provide information regarding the heart's mechanics and hemodynamic function. There are four main modes of echocardiography: brightness mode (B-mode), motion mode (M-mode), Doppler imaging, and three-dimensional (3-D) echocardiographic imaging. Echocardiography can provide comprehensive information on cardiac anatomy, physiology, and mechanical properties. In humans, echocardiography consists of transmitting high-frequency sound waves, which are reflected off different tissue moieties (eg, myocardium, blood, valves, etc.) back to an ultrasound transducer, which receives the reflected signal of all tissues. Software dynamically processes the incoming signals from the different tissues and generates a real-time image based on the known acoustic impedances of each tissue. B-mode produces 2-D views of the heart (short or long axis), allowing the assessment of cardiac chamber dimensions, physiology, and visualization of cardiac anatomic structure such as papillary muscle and valves. M-Mode relies on a rapid succession of B-mode scans along a single axis displayed over time to produce images that appear as a continuous tracing, to indicate motion.

The introduction of Doppler technology to echocardiography has revolutionized this technique. Doppler's general principle in echocardiography is based upon measuring the changes in the frequency of the backscatter from the ultrasound beam signal produced from small moving structures (ie, red blood cells, RBC). The change in frequency is called the Doppler shift and the magnitude of the Doppler shift (in frequency) is proportional to the velocity of blood cells. In contrast, the polarity of the shift is determined by the direction of blood flow toward (positive) or away from the transducer (negative).[47] Doppler echocardiography is used to measure and assess blood flow through the heart's chambers and valves. Doppler echocardiography can thus detect abnormal blood flow within the heart (or larger vasculature), which may indicate a dysfunction of the heart's four valves or walls.

Doppler echocardiography is presently the most powerful tool for assessing cardiac function in chick embryos, in vivo.[30] Several studies described hemodynamic alteration in the developing chick embryonic heart, and both

TABLE 1 Evolution of blood flow velocity during embryonic developmental stages of chick using Doppler OCT Doppler ultrasound, or μ-PIV.

References	System (mode)	Stage	Investigated region	Peak Velocity (cm/s)	Conditions
Hu and Clark[48]	Doppler (20 MHz)	HH18	Vitelline artery	0.26	Normal
		HH21		0.39	
		HH24		0.61	
		HH27		1.13	
Broekhuizen et al.[58]	Doppler (20 MHz)	HH20	Vitelline artery	2.01	Normal
		HH24		2.61	
		HH27		4.50	
		HH29		4.91	
		HH31		7.01	
		HH35		8.25	
Bharadwaj et al.[53]	Doppler (40 MHz)	HH23	Proximal	19.0	Normal
		HH27	Distal	21.0	
		HH30	RVOFT	62.0	
		HH30	LVOFT	53.0	
Nakazawa et al.[49]	Doppler (20 MHz)	HH21	Vitelline artery	0.34	Normal
Yalcin et al.[52]	Doppler (40 MHz)	HH17	AV Canal	3.0	Normal
		HH23		12.0	
		HH27		40.0	
		HH30		45.0	
Yoshigi et al.[119]	Doppler (20 MHz)	HH24	Vitelline artery	0.90	Normal
Benslimane et al.[30]	Doppler	HH26	AV valve and OFT	44.2	Normal
Butcher et al.[62]	Doppler	HH21	AV canal	8.1/4.84	Normal/LAL
			L-AV canal	38.3/30.4	
			R-AV canal	48.9/45.4	
Sharma et al.[120]	Doppler	HH21	Vitelline artery	0.75/0.62	Normal/ hypoxic
Davis et al.[36]	Doppler OCT	HH17	Peripheral vessel 1	3.1	Normal
Stekelenburg-de Vos et al.[121]	Pulsed Doppler meter	HH17	Right lateral vitelline vein	2.8	Normal
Clark and Hu[7]	Pulsed Doppler	HH18	Vitelline artery	2.6	Normal
Davis et al.[36]	Spectral Doppler velocimetry	HH17	Vitelline artery	1.55	Normal
Rugonyi et al.[81]	Spectral domain OCT	HH18	Outflow tract	1.78	Normal
Yalcin[117]	Two-photon guided line scanning	HH24	Vitelline artery	1.67	Laser ablation

Abbreviations: AV, atrioventricular; HH, Hamburger & Hamilton; LVOFT, left ventricular outflow tract; OCT, outflow tract; PIV, particle image velocimetry; RVOFT, right ventricular outflow tract.

physiological and pathological conditions have been studied using Doppler echocardiography[48-51] to resolve the architecture and flow characteristics in the embryonic chick AV canal and OFT.[52,53] These systems have multiple modalities including B-mode, M-mode, Doppler, color flow and tissue strain that maximize the ability to visualize and extract data from cardiac tissues in small model organisms in vivo.[54] Indeed, several Doppler echocardiography (single mode) platforms mainly used for rodent imaging were successfully applied to chick embryo studies, thus providing a low-cost option for simple flow measurements.[30] Combined with a pressure

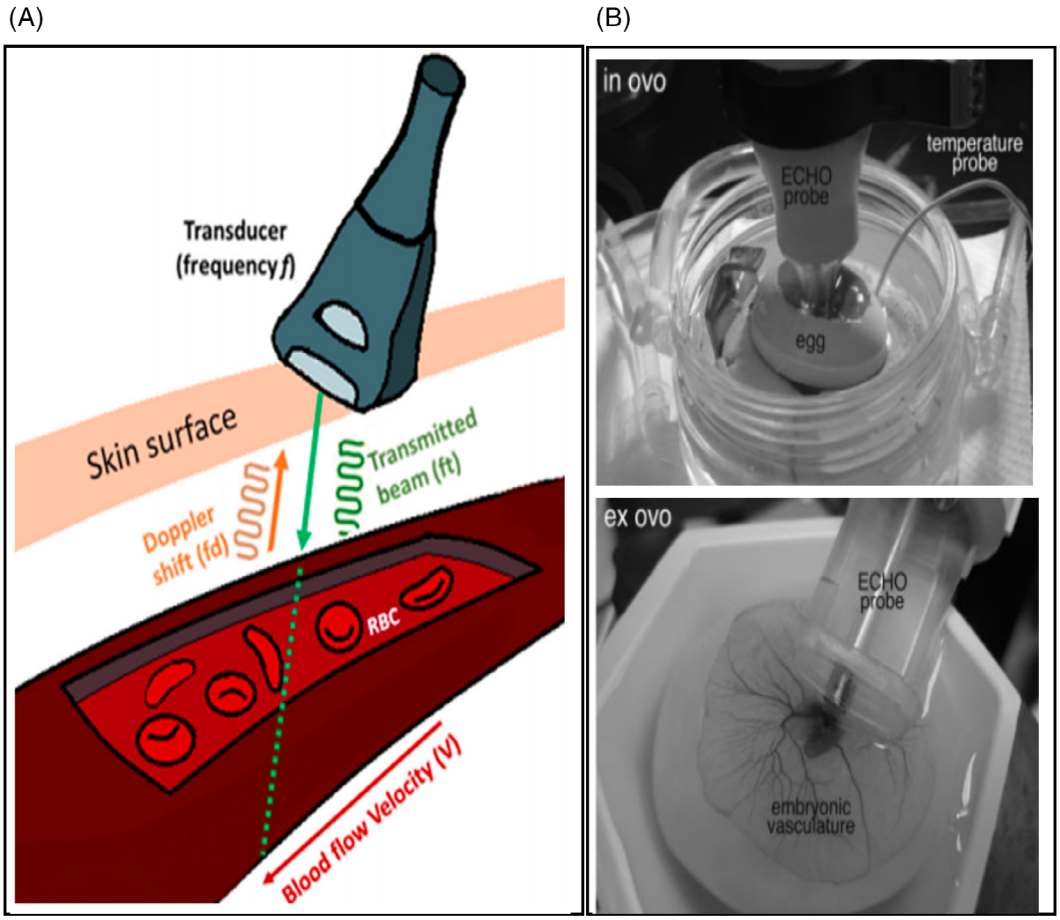

FIGURE 2 Doppler echocardiology for in vivo use in chick embryos. A, Doppler mode blood flow measurement principle. *Source*: replicated from Benslimane et al.[30] with permission. B, Avian ultrasonographic imaging setup. Top: Probe size relative to the egg (in ovo imaging); bottom: cultured embryos ex ovo at the stage of HH 24 and 29. *Source*: replicated from McQuinn et al.[57] with permission.

measurement technique, simultaneous flow signals can be modeled together to collect a pressure-volume loop data (PV loops).[50,55,56] However, applicable pressure measurement techniques are largely invasive, thus limiting the applicability of the pressure sensing techniques. Commercial Doppler Echocardiography systems are available with a typical minimum frequency of about 10 MHz. The maximum frequencies are near 90 MHz; however, the BFV is measured from 7.5 to 40 MHz (Table 1). Therefore, graphical representations of flow must be obtained using modalities that operate within range to produce spectral data (waveforms). Depending on the Doppler mode, spectral data are generated as per Equation (1) with the probe positioned as shown in Figure 2A,B to align with the flow direction.

$$\text{Doppler frequency (Fd)} = 2 \cdot \text{Ft} \cdot V \cdot \cos = \frac{\theta}{C}. \quad (1)$$

The dynamic nature of the produced waveform indicates BFV and reflects the elasticity of heart chambers and blood vessels. Once positioned, these systems can be easily tuned to obtain waveforms that allow monitoring and analysis of cardiac function.

1.2.1 | Doppler echocardiography for measuring flow velocities in chick embryo

The ability to study BFV in embryos provides powerful experimental tools to study the development of cardiac function in small experimental animals and chick embryos[57-59] (Figure 3). We have investigated the AV canal and OFT in several[30,52,53] that highlight the efficacy of Doppler echocardiography in chick embryos.

In these works, we measured the AV orifice diameter and recorded peak velocity at the midline of the valve.[57,61] We later measured the inflow velocity to the AV and OFT canal for cultured chick embryos using Doppler ultrasound (Visualsonics, Figures 4 and 5).[52,53] Importantly, in addition to providing a platform for studying normal blood flow velocities in a developing

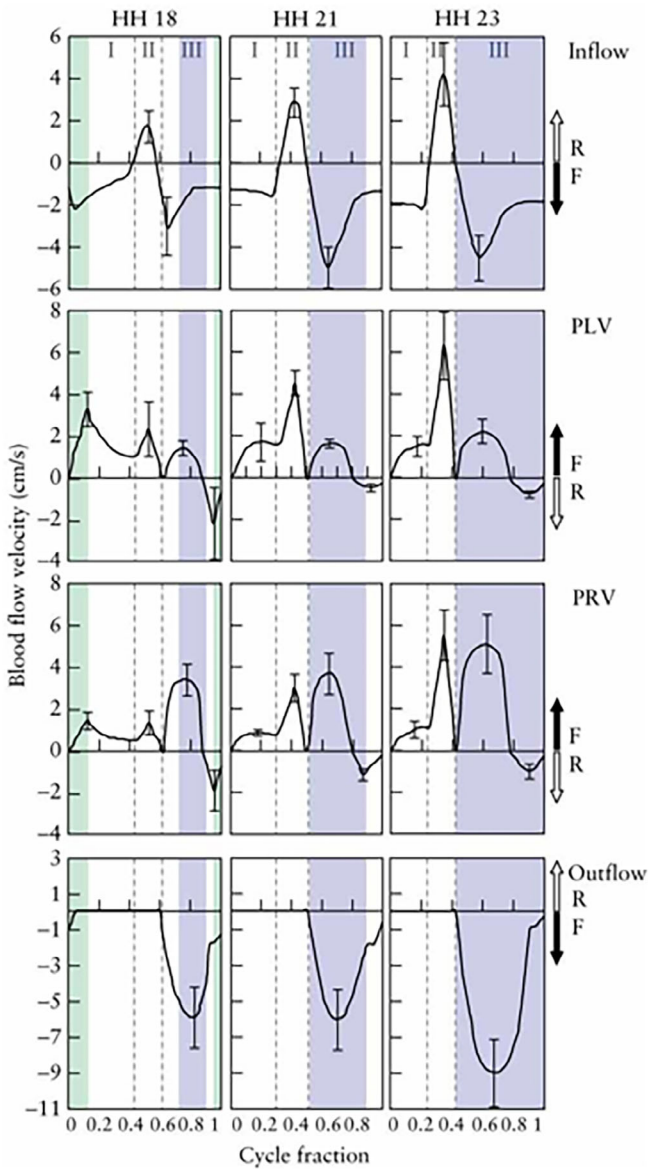

FIGURE 3 Different stages of (HH 12, 21, and 23) BFV waveform at various locations. Different ventricular phases during one cardiac cycle (Areas I—passive filling; II—active filling, and III—ejection phase; forward [F] and reverse [R] direction of flow). Blue bars in the background indicate the closure time of the AV cushions and the shaded green bars indicate the closure time of the outflow cushions. *Source*: adapted from Oosterbaan et al.[60] with permission.

chick embryo at fine resolution, Doppler ultrasound also allowed us to study the hemodynamics of CHDs modeled in chicken heart through surgical interferences.[51,60] For example, recently, we demonstrated that surgical interference (left atrial ligation) affected hemodynamics and induced clinically relevant cardiac disease morphologies.[62] In a following study, we introduced a new surgical approach called right atrial ligation to study the influence of right-side flow disturbance in chick embryo heart development 15.

Several studies have demonstrated that abnormal BFV patterns cause myocardial structural defects.[9,60,63] For example, hemodynamic overload alters OFT collagen distribution during early embryonic development and contributes to cardiac dysfunction (Figure 6).[64] Hemodynamic modification by changing blood flow through surgical intervention has been well-demonstrated in the chick embryo.[65] These microsurgeries were performed on embryonic 3–4 days, when the heart is most sensitive to hemodynamic alterations.[66] Another surgical technique used in chick embryos is ligation of the vitelline veins to reduce blood flow to the heart, and conotruncal banding to narrow the OFT.[67,68] Permanent obstruction of the right lateral vitelline vein with a microchip causes alterations in intracardiac blood flow velocities and eventually results in specific cardiovascular malformations.[69] Our work has followed suit with development of left atrial ligation (LAL) procedures that pair with measurement of BFV in chick embryos.[30,65,70] Such microsurgical techniques clarify how morphological deviations in cardiovascular development might cause aberrant hemodynamic patterns that translate to cardiovascular dysfunction.

1.2.2 | Advantages/limitations

Doppler echocardiography imaging systems can rapidly acquire images at 100 frames/s (Vevo2100's/Vevo3100's) with ongoing improvements in sensitivity.[9] However, Doppler echocardiography imaging systems are susceptible to high noise. Further, longer wave ultrasound penetrates deeply, with low resolution, whereas shorter wavelengths have less penetration into tissues, with higher resolution to resolve smaller objects. Thus, tradeoffs exist between achieving deep tissue penetration and high sensitivity to resolve small structures and features in the tissue. Thus, advancements that enhance spatial resolution will increase our detection limit for assessing fine details in these tiny, venerable model organisms.[61]

1.3 | Doppler OCT

OCT is a form of interferometry that produces micrometer-resolution images of optically scattering materials by interpreting the scattering of low coherence light across different materials[71] and is capable of penetrating relatively deeply into tissues. In cardiology, OCT can be used to image coronary arteries to determine their lumen morphology and microstructure.[72] Doppler OCT analysis relies on detecting a phase shift in values between adjacent

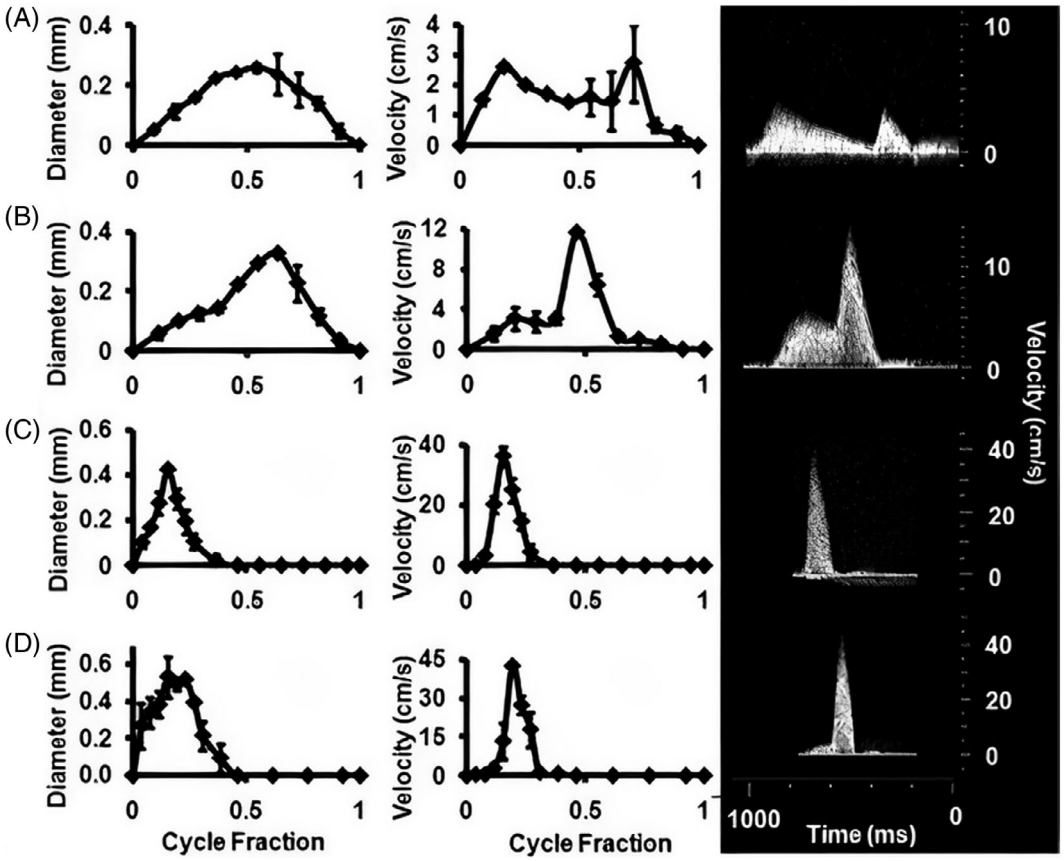

FIGURE 4 Ultrasound measurement of atrioventricular (AV) orifice diameter (panel left) and velocity (panel right) during different stages. Right side panels are Doppler velocity measurements of different embryonic stages (Hamburger & Hamilton). A, 17; B, 23; C, 27; and D, 30. AV canal velocity correlation with left atrial input velocity for stages. *Source*: acquired from Yalcin et al.[52] with permission.

in-depth OCT scans at each point, caused by the movement of scattered light. The velocity component is quantified in the direction of the light beam.[73] Thus, the pairing of this methodology allows the calculation (and visualization) of BFV with superior spatial and temporal resolution. In cardiology, for example, OCT is used to image deep into the heart tissue into coronary arteries to examine lumen morphology and microstructure,[72] and is applied in chick embryology.[36] In contrast to Doppler echocardiography, OCT relies on light and natural optical properties of thin, semi-transparent tissues and it provides far better resolution at 2 μm and adequate penetration depth, depending on the tissue properties. Despite their differences in sensor technologies, Doppler modalities and OCT can be paired to simultaneously acquire Doppler images alongside structural OCT images.

1.3.1 | Doppler OCT for measuring flow velocities in chick embryo

OCT has revolutionized live bioimaging in small organisms largely because the technique is so effective for assessing functional morphology of tissues. Doppler OCT is a powerful extension of OCT, for visualizing and measuring blood flow.[74] In a noteworthy study, Huber et al., revealed a new OCT technology (Fourier-domain OCT) which includes spectrometer-based spectral-domain OCT, enabling a leap in higher imaging resolution and image quality.[75,76] Recently, Jenkins et al., established an application to study heart dynamics in four dimensions in the chick embryo through high-speed OCT imaging.[77] In addition to structural imaging, OCT can be used for Doppler analysis to obtain detailed velocity measurements from moving structures with high resolution.[78] Such BFV data sets can be used to model dynamic blood flow-related processes that occur during early embryonic development[79] and to provide detailed depictions of flow characteristics down to the capillary-level.[80] Rugonyi et al. showed fine details of cardiovascular function using spectral domain OCT to visualize and quantify blood flow velocities in the chick embryo and changes in cardiac wall motion under normal and altered hemodynamic conditions,[81] while Ma et al. demonstrated a new method to quantify the absolute BFV in the early-stage OFT.[82] Doppler OCT technology enables simultaneous

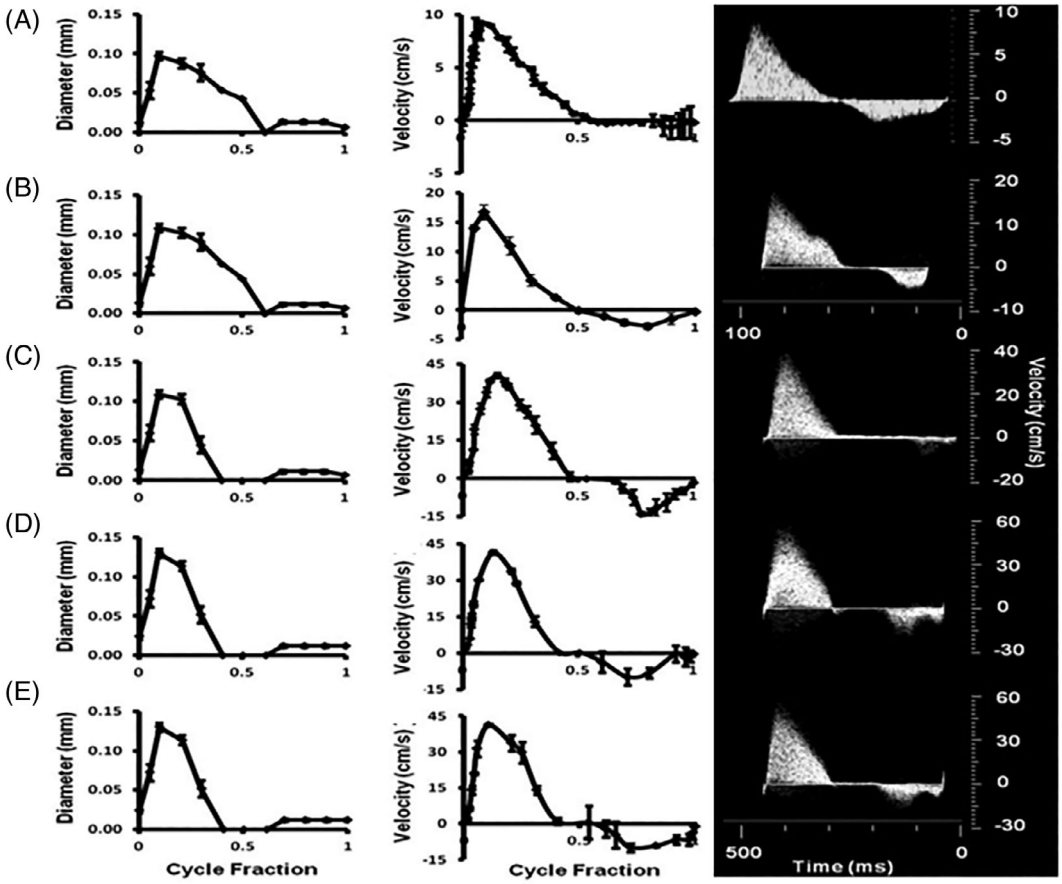

FIGURE 5 Ultrasound measurement of stage-specific outflow tract (OFT) diameters (left panel) and OFT orifice flow profiles and (right panel). Velocity recording at different embryonic (Hamburger & Hamilton) stages A, 16; B, 23-proximal; C, 27; D, 30-LVOFT; and E, 30-RVOFT. RVOFT, right ventricular outflow tract; LVOFT, left ventricular outflow tract. *Source*: adapted with permission from Bharadwaj et al.[53]

correlation of blood flow with the dynamic expansion and contraction of the heart tube. Thus, investigators with Davis et al., were able to acquire BFV from three blood vessels in an HH17 chick embryo using in vivo Doppler and 3D OCT techniques[36] (Figure 7).

1.3.2 | Advantages/limitations

The most significant advantage of Doppler OCT is that BFV measurements can be spatially and temporally resolved and correlated with the 3D structure of the embryo. Larina et al., demonstrated that embryo image acquisition was performed at 512 A-scans (comprising image 4–6 mm wide) per frame without averaging, which resulted in the acquisition rate of 28 frames per second.[37] Such temporal resolution is at normal video frame rates (25–30 fps.). In addition, increasing the frame rate can be achieved in part by decreasing the A scans per frame, which resulted in precisely viewing the field of interest. Further, in a recent study, it was possible to acquire 4D OCT images from embryonic Wdr19 mutant mouse hearts,[83] showing the possibility of 4D imaging in chick embryo hearts. Noting the rapid advancements in computing and imaging technologies, OCT has the potential to become a valuable tool for studying developmental physiology in small model organisms like chick and zebrafish embryos. Further, OCT has been shown to have a depth penetration of only a few millimeters preventing working with older chick embryo heart scanning. Likewise, light penetration along the axial plane also poses a barrier to enhancing spatial resolution.

1.4 | Micromagnetic resonance imaging (μMRI)

μ-MRI is a powerful technique that uses radio waves and magnetic fields in for high resolution medical imaging.[84] By monitoring the interaction between the magnetic field and the spin of the atomic nuclei, μ-MRI techniques are capable of imaging fine structural details and has been

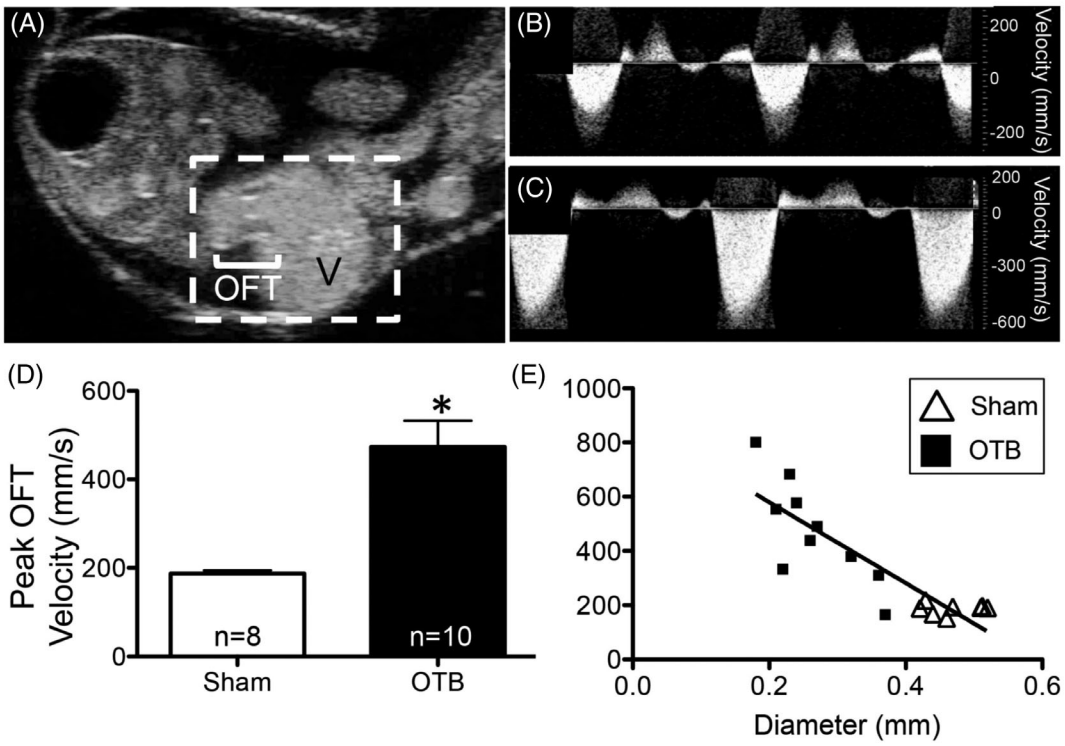

FIGURE 6 Blood flow velocity (BFV) measurement by ultrasound imaging for outflow tract (OFT). A, Embryonic stage 24 chick heart B-mode image (hatched white box). Blood flow were observed from the ventricle through OFT. BFV after OFT from control (B) and outflow tract banding (OTB) to obstruct the flow of the OFT (C) Embryos. Peak OFT velocity marginally increased in OTB embryos (D). * $P < 0.05$ via *t*-test. The graph shows the diameter of the OFT vs BFV (E). *Source*: adapted from Rennie et al.[64] with permission.

applied for use in small model organism research. Cardiovascular μ-MRI allows non-invasive evaluation of the function and structure of the cardiovascular system,[85] and is used in the detection of cardiac diseases such as CHDs,[86] valvular heart disease[87,88] and cardiomyopathy.[89,90] Moreover, μ-MRI can be used for diagnosing diseases related to the structural defects in the aorta, including aneurysms, coarctation, dissections, and for analyzing the pulmonary veins.[91-95]

Chick embryo μ-MRI imaging was established in the 1980s when Bone et al. revealed the first three-dimensional MRI image of a live chick embryos.[96,97] The technique was adapted as μ-MRI and first used regularly on small animals between 1994 and 1996 by Smith, Johnson and co-workers at Duke University.[98,99] Over a decade later, Bain et al. used μMRI to non-invasively monitor development and growth of individual organs, including brain, liver, and heart, in the chick embryo, starting at 12 days of incubation.[100] More recently, others have been able to apply this MRI technology to track brain development in nearly histological serial sections, in vivo (Figure 8).[101] Goodall et al. demonstrated well how high-resolution μ-MRI can measure subtle morphological changes following experimental manipulation of eye development in the chick embryo. Their results demonstrated that μ-MRI is an essential tool for rapid and sensitive characterizing normal chick ocular development and morphology in experiments that examined the potential effects of surgical or genetic manipulations of chick embryo eyes *in ovo*.[102] Indeed, the resolution and applications suggest that this powerful technique can be used for chick embryo cardiac research. Beyond high resolution imaging of soft tissues, flow μ-MRI is a modality used to measure blood flows, and was previously adapted for imaging mouse embryos.[103-105] Noting that the above techniques described in this short review were all also adapted from mouse embryo protocols, it is probable that flow μ-MRI techniques will be adapted for chick embryos. Further improvements in technology and software enhanced spatial resolution to enable investigators to quantify several cardiac variables (in ovo).[106-108] Additionally, Herrmann et al., performed time of-flight MR angiography imaging in chick embryos, but encountered reduced blood flow and reported image acquisition difficulties while using their cooling protocol.[109]

1.4.1 | Advantages/limitations

MRI imaging provides enhanced soft-tissue contrast, 3D anatomical information and high spatial resolution. Investigators continue to show that μMRI is suitable for

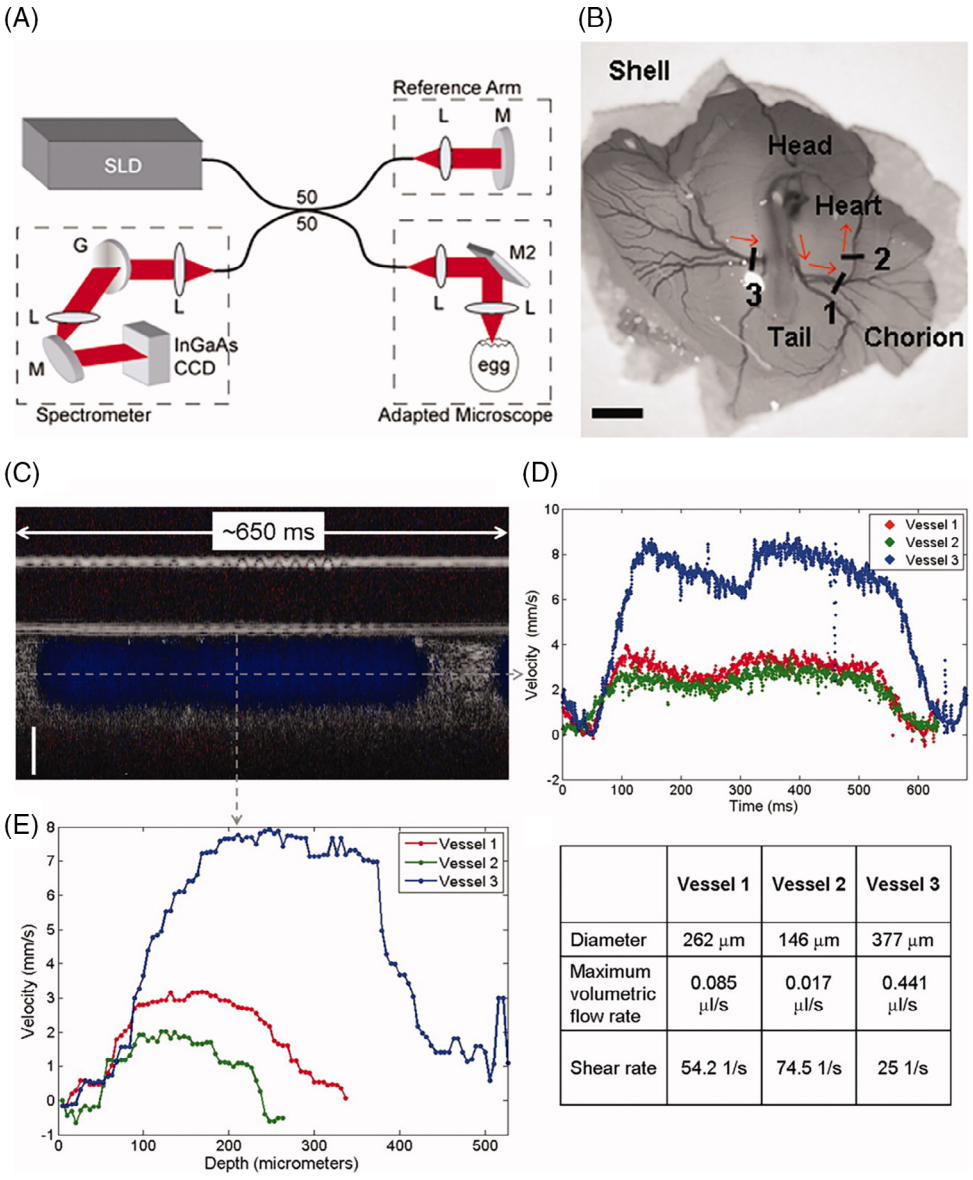

	Vessel 1	Vessel 2	Vessel 3
Diameter	262 μm	146 μm	377 μm
Maximum volumetric flow rate	0.085 μl/s	0.017 μl/s	0.441 μl/s
Shear rate	54.2 1/s	74.5 1/s	25 1/s

FIGURE 7 Blood flow measuremnts from three extraembryonic vessels using optical coherence tomography (OCT). A, OCT experimental setup. B, location of measured blood vessels. C, vessel 2 superimposed M-mode images obtained from Doppler and OCT scans. D, blood flow velocity dynamics of three vessels. E, velocity profiles (left) and Doppler diameter, flow, and shear stress measurement (right) for three vessels. *Source*: replicated from Davis et al.[36] with permission.

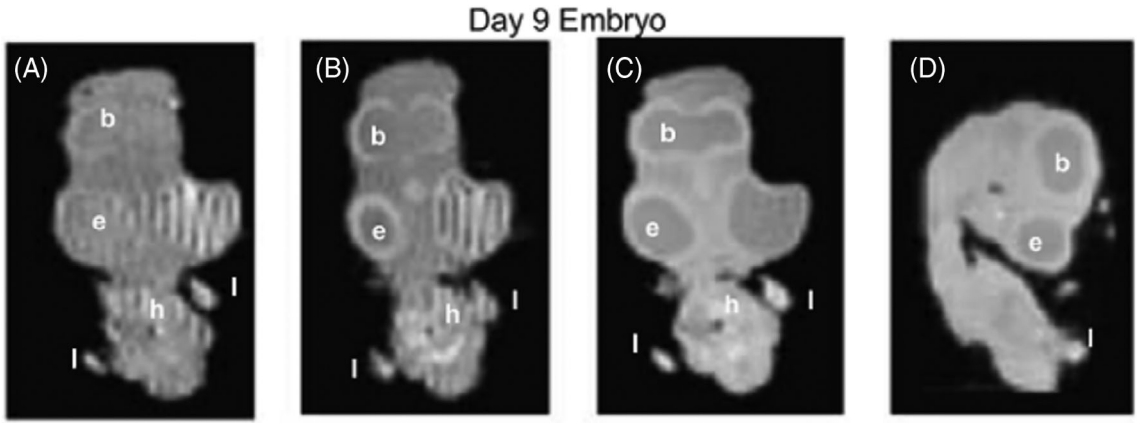

FIGURE 8 μ-MRI images of the chick embryo. A–D, day 9 embryos spin echo images (e, eye; h, heart; b, brain; l, limb). *Source*: adapted from Zhou et al.[101] with permission.

the three-dimensional visualization of small structures, in near real time.[110] Indeed, reports continue to show enhanced application for MRI technologies in research diagnostic imaging.[109,111] However, any MRI technique is limited by high equipment costs, and equipment availability[112] limiting its applicability.

1.5 | Microscopy techniques

Under magnification, blood flow can be visualized through the (mostly) transparent embryonic vasculature and cardiac structures. When successive images are filmed as video, BFV in chick embryonic heart or blood vessels can be calculated by first identifying the RBCs in the images, then measuring the distance each RBC moves between images in the video. Each RBC velocity is calculated as a distance per unit time, which equates to BFV. This technique is commonly applied to measure microscale velocity fields, and is known as microparticle image velocimetry (μ-PIV).[113-115]

Chen et al. combined μ-PIV with OCT to quantify the blood flow in an arterial vessel in chick embryos.[116] The major advantage of combining these techniques is that it provides accurate and in-depth flow assessment on embryonic animal models and fills an essential gap in quantitative microscopic velocimetry techniques. Line scanning is more potent than classical μ-PIV that is applied with a confocal, two-photon, light sheet microscope or with OCT to image into chick embryo heart. The penetration depth is only a few mm, making it difficult to fully image the heart at depth, but we have used a two-photon guided line scanning approach to measure vitelline vessel blood velocities in HH24-HH25 stage embryos with success.[117] Using this technique, we showed flow distribution within the vitelline network following clotting one vessel within the network via nonlinear femtosecond laser photoablation.[117] This technique uses a longitudinal line scan centered on RBCs in the imaged vessels to capture fluorescent vessels. Each subsequent scan is displayed below the previous one, forming a space-time image in which time increases from top to bottom. As the non-fluorescent RBCs move, dark streaks appear in the images. The velocity of RBCs is calculated from the slopes of these dark lines, which is inversely proportional to the slope of the lines.[117] Further, Chen et al. used OCT guided line scanning approach applied to arterial blood vessels of the chick embryo[116] (Figure 9). These techniques continue to provide a promising tool for monitoring disease progression in these small model organisms.

1.5.1 | Advantages/limitations

The key advantages to μ-PIV are better resolution and measurement accuracy than other flow measurement techniques, including, molecular tagging velocimetry and microlaser Doppler velocimetry.[118] Image quality is another major limitation, mostly restricted in this application by tissue opacity. Indeed, as pigment forms and tissues thicken during development, imaging depth is further reduced in the chick embryo. Indeed, we found that the maximum working depth in the chick was near 1.8 mm, which precludes this application for embryos older than HH27.[117] PIV techniques are further labor intensive since μ-PIV workflow generally dictates that images are acquired in the laboratory, then analyzed later. However, the popularity and reliability of μ-PIV data resulted in commercial applications within several microscopy software suites and led to opensource code for ImageJ and other freeware resources. Unfortunately, these software analyses are mostly slow and not ideal for real-time flow measurement. Advances in microscopy and image processing will soon allow these software-based techniques for high-speed user-defined scans for

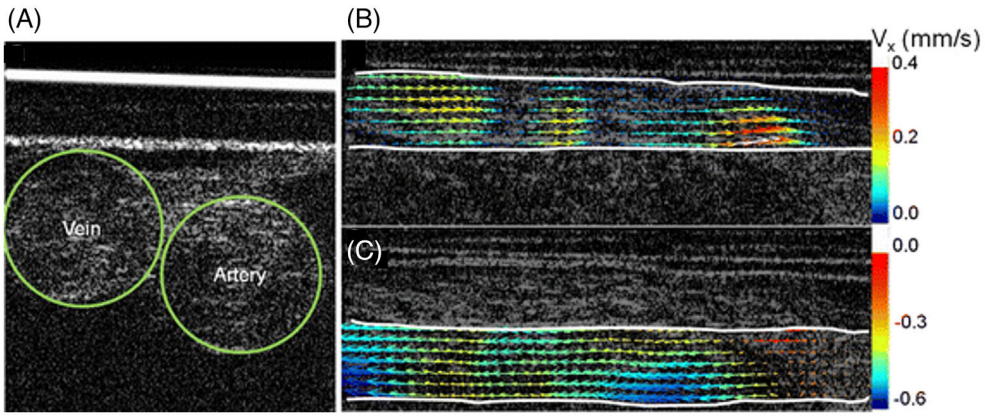

FIGURE 9 HH18 stage Embryonic chick flow assessment of arterial and venous blood via OCT-μPIV technique. A, two vessels overlapping view. B and C, depth resolved velocity fields were calculated from two vessels. Green outline is a vessels boundary (A) and white (B and C) solid lines. *Source*: adapted from Chen et al.[116] with permission.

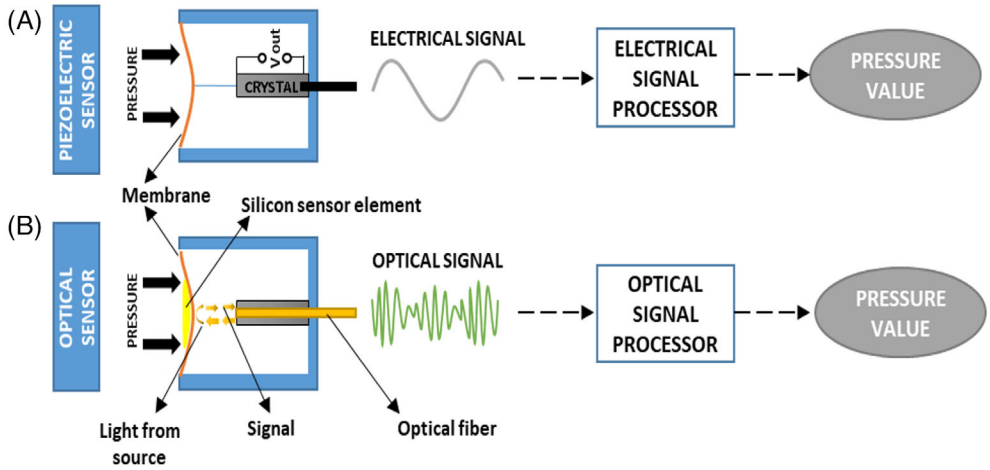

FIGURE 10 Working principle of: A, piezoelectric sensor; B, optical sensor, for pressure measurement.

near-simultaneous measurement of RBC velocity. Such advances are concurrent with the high cost of research-grade microscopy.

1.6 | Measurement of blood flow velocities in chick embryo using different techniques

The abovementioned techniques have been utilized to measure blood flow velocities for different-stage embryos. Below table summarizes overall, the BFV changes (HH12 to 31) during development that were measured with Doppler OCT, Doppler ultrasound, or micro-PIV (Table 1).

2 | MEASUREMENT OF BP

Since BP provides the driving force for blood flow, it is a critical variable for cardiovascular health, techniques have been developed to measure BP in popular model organisms. However, conventional pressure measurement techniques cannot accurately measure the small pressures in the tiny blood vessels of the chick embryo. Sensitive piezoelectric and optical manometer systems are commonly adapted for use in the larger vasculature and heart in the chick embryo. For smaller vessels, however, the-servo-null technique must be used. for small vessels. for small vessels, the servo-null technique must be used.

2.1 | Direct pressure measurement with catheters

Direct pressure measurement via catheter is achieved by connecting a fluid-filled catheter between the vasculature and a pressure transducer (Figure 10). As the pressure in the vasculature changes, the force is transmitted through the catheter to a deformable membrane in the transducer. The degree of deformation of the membrane is measured using either a piezoelectric or optical sensor that outputs a voltage signal proportional to pressure within the vasculature. Catheters can be hand pulled from polyethelene tubing to create microcatheters for very small vessels. The sensors are used in the microcatheter technique differ according to the type of catheter used.[122] The diaphragm in piezoelectric sensors moves with the effect of pressure, and this change creates a voltage difference in the crystal in the sensor. The generated voltage is processed in the signal processing unit to determine the dynamic pressure values. Piezoelectric sensors are sensitive to measuring dynamic and slight changes in pressure but are not well suited to monitor static pressure due to several issues with the design that result in a leak, over time. The diaphragm structure of optical sensors used in microcatheters is similar to the ones in piezoelectric sensors. Pressure is measured in optical sensors that monitor a phase delay induced as the optical membrane deforms from the effect of BP, unlike piezoelectric sensors that report the voltage difference created by the force acting on the membrane (Figure 10). Also, optical sensors are not affected by electrical interference, do not conduct electricity, and are rarely affected by temperature and humidity, which causes signal deviation relative to piezoelectric sensors.[123]

Several studies have used fluid-filled catheter pressure measurement techniques in chicken embryos. Previous studies measured chick embryonic arterial blood pressure using small volume mechanical transducers.[41,124] Investigators modified techniques to access the smaller vessels and measured the distal vitelline artery pressure using analog signal processing to compensate for pressure

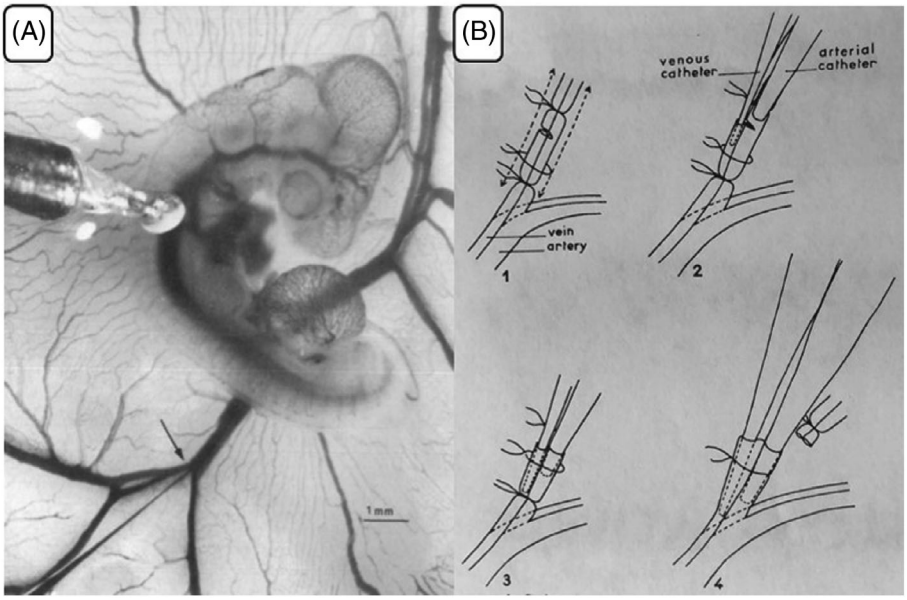

FIGURE 11 Cardiac pressure measurement in the chick embryo. A, 5 μm in diameter pressure pipette was inserted into the HH21 stage chick embryo left vitelline artery. B, Catheterization of an artery/vein of the embryo after 7 days of incubation. *Source*: adapted from Clark and Hu[7] and Girard[40] with permission.

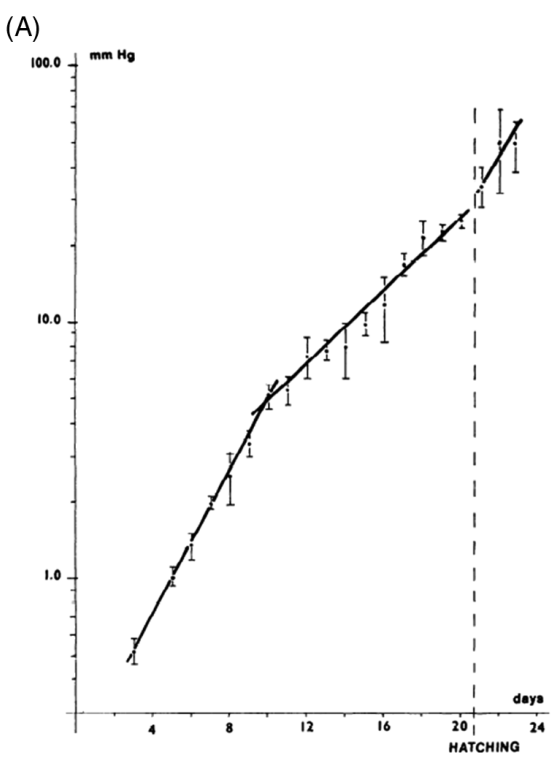

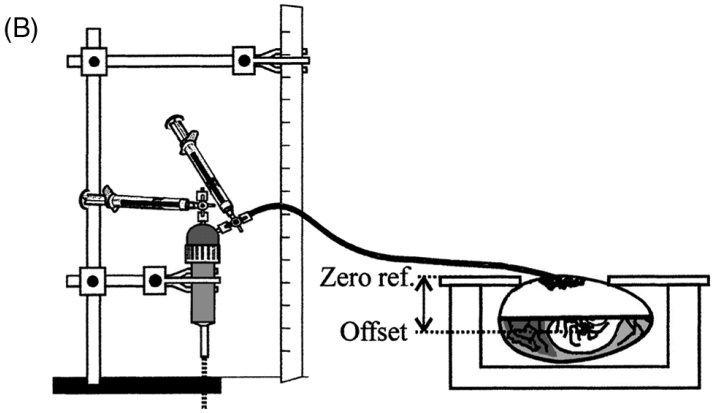

(C)

Days of Incubation	Strain	MAP
9	WL	1.01 ± 0.02 (3)*
12	WL	1.08 ± 0.08 (4)*
15	WL	1.15 ± 0.08 (5)*
18	WL	2.22 ± 0.17 (6)†
19	WL	2.68 ± 0.29 (4)†
19	Ply	2.40 ± 0.21 (8)†
20	Ply	2.80 ± 0.13 (9)†
21	Ply	3.18 ± 0.28 (9)†
Hatch	Ply	2.40 ± 0.33 (5)†

FIGURE 12 Catheter cardiac pressure measurement in chick embryo. A, mean arterial pressure in growing chick embryo.[39] B, schematic drawing of experiment setup used in manometer system.[42] C, mean arterial pressure (kPa). WL, white Leghorn strain; Ply, plymouth strain.[42]

distortion from a miniature diameter glass pipette connected to a mechanical pressure transducer.[41] Another study investigated the ventricular pressure in relation to intracapillary pressure in ED2 to ED7 chick embryos (HH17-HH30).[124] High ventricular pressure was recorded for ED5 (HH26).[41] Clark et al., measured aortic BP by inserting a pipette into the HH21 stage chick embryos (Figure 11A).[7,41] As investigators became proficient in these techniques, several demonstrated chronotropic sensitivity effect to sympathetic stimulation on chick embryos using the microcatheterization technique (Figure 11B).[39]

Importantly, Girard's landmark (1973) study used a manometer system with thin glass catheters with an outer diameter of 0.15–0.40 mm, somewhat thinner than the arteries, to assess arterial BP in 600 leghorn embryos aged 3–20 days and 65 chicks aged hatching to 3 months. Figure 12A shows the mean arterial pressure measurement results of 3–20 days for embryonic and 3 h to 3 months for the posthatch chick.[39] Altimiras et al. conducted a similar study in which they measured the arterial pressure of 9–21 days old Leghorn, 19–21 days old Plymouth embryos, and Plymouth hatchlings using the manometer system, the experimental diagram of which is shown in Figure 12B. The mean arterial BP measurements of the embryos and hatched chicks are demonstrated in Figure 12C.[42] In addition to these studies, arterial[125,126] and ventricular pressures[127,128] were measured in chick embryos at various day-old intervals using experimental settings built with comparable thin glass catheters and manometer devices.

2.2 | Indirect pressure measurement using electrolyte solutions

Another approach to measuring BP in developing chick embryo is the servo-null micropressure technique using the 900A Micropressure System (World Precision Instruments). The servo-null technique measurement principle is based on the maintenance and measurement of an ion gradient within a glass microelectrode using electrophysiological technique. The small microelectrode (2Altimiras5 μm diameter) can be inserted into any fluid-filled space to measure pressure. Once the microelectrode is prepared, the electrical resistance measured at zero pressure is set as the null value. If the pressure in the space (eg, artery) changes, the force exerted on the microelectrode will offset the volume of electrolyte fluid within the microelectrode, which is constantly measured as electrical resistance. The 900A Micropressure system will automatically counter the force in just a few milliseconds, bringing the resistance back to its

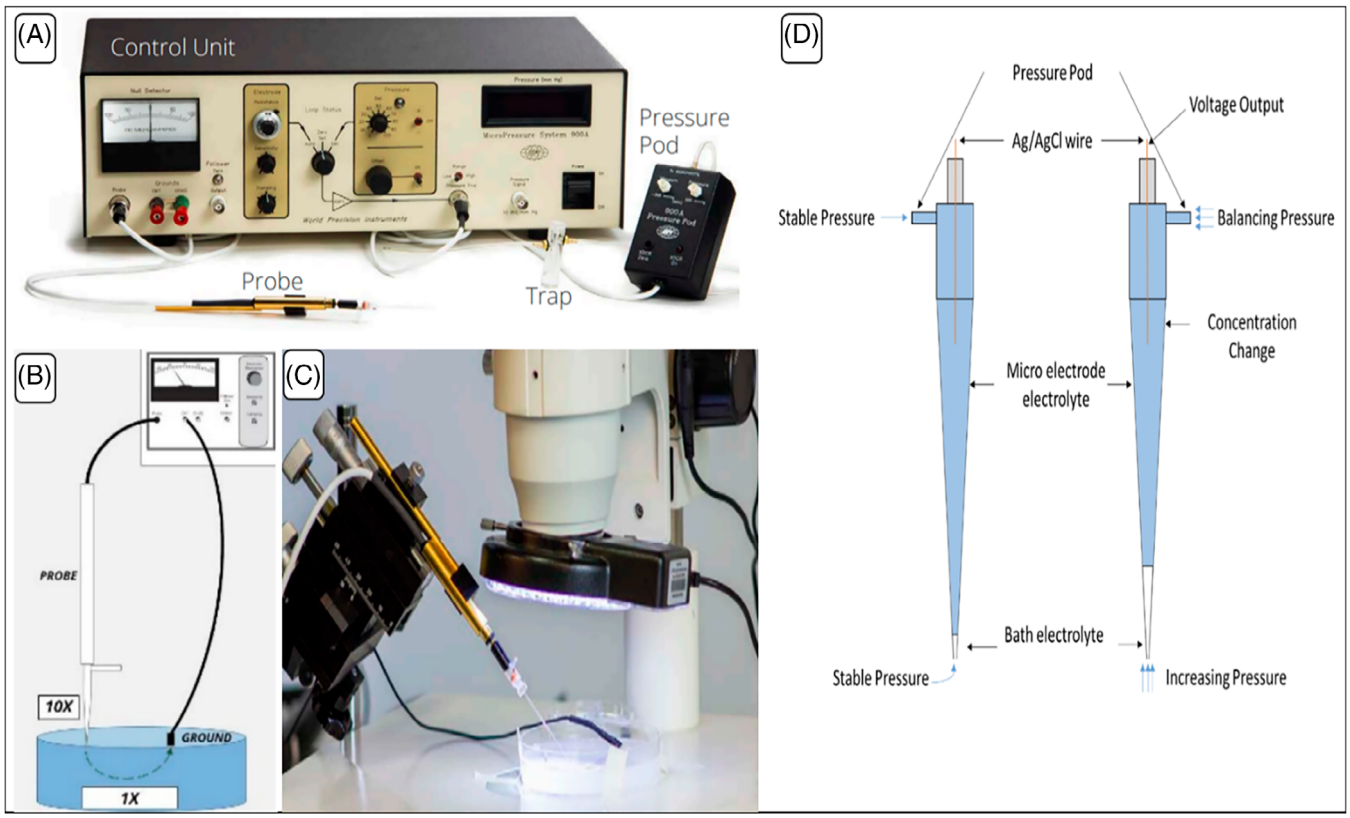

FIGURE 13 900A microelectrode pressure system and its principle. A, the 900A micropressure system includes the control unit, probe, pressure pod, vacuum trap, and null detector. B, the circuit is complete when the reference electrode is immersed in the solution at the measurement area, which is connected to the micropressure system. C, the probe is mounted on the micromanipulator and the tip is advanced to the measurement site (chick embryo vitelline artery). D, The micropressure system uses a micropipette that is inserted in the vasculature for the measurement of pressure.

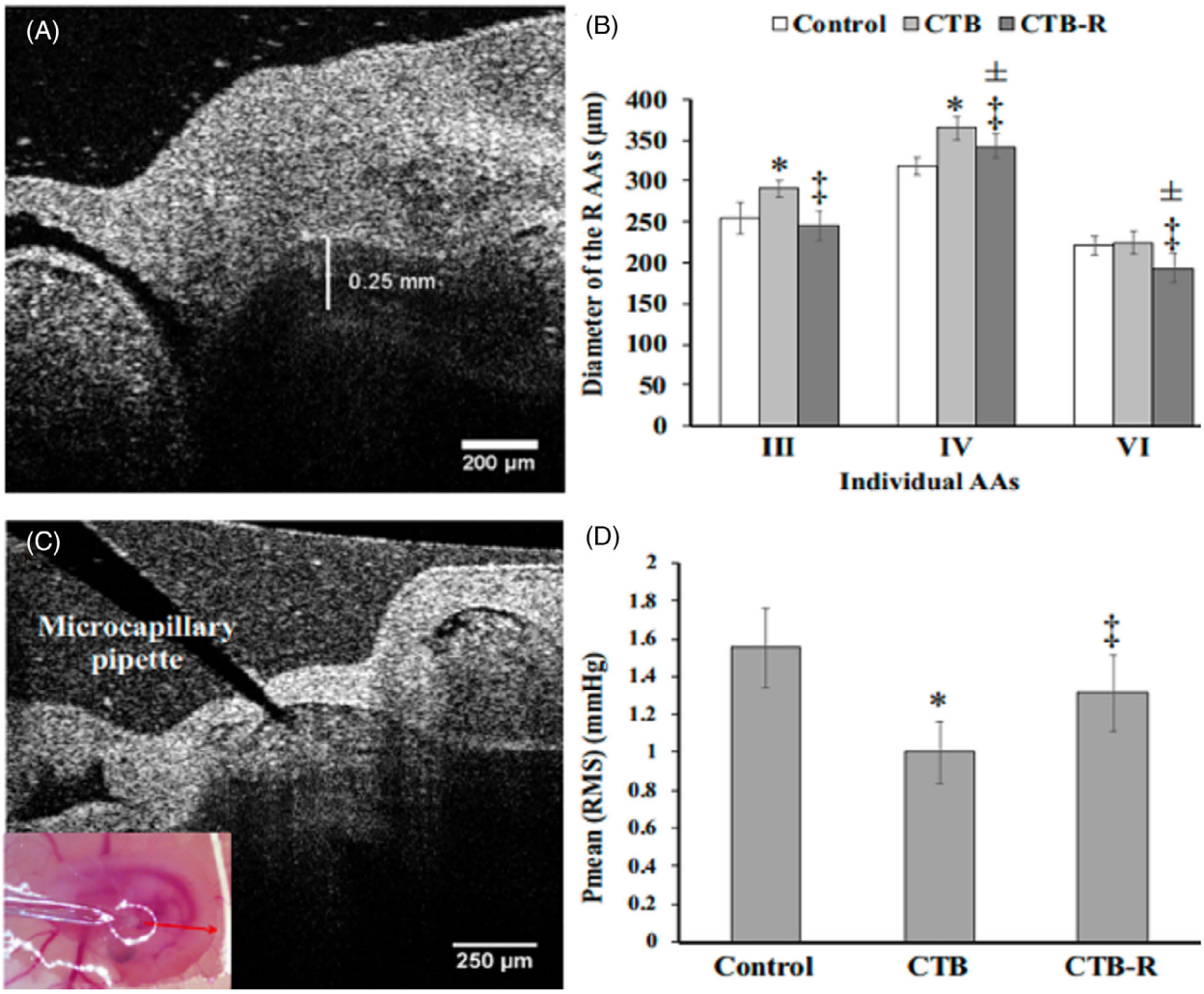

FIGURE 14 Optical coherence tomography (OCT) guided measurement of blood pressure (BP) and diameter of aortic arch (AAs) at the stage of HH24. A, diameter of the AAIII (red line). B, changes in diameter of individual AAs ($n = 10$). C, BP measurement using OCT guided microcapillary pipette. D, repeated pressure measurement ($n = 10$). Groups: control, CTB: conotruncal banding and CTBR (conotruncal banding release). *Source*: replicated from Celik et al.[133] with permission.

null value, using external pressure and a vacuum source, connected to a highly sensitive valving system. The amount of offset required to bring the value back to the null resistance is proportional to the pressure sensed at the tip. As the system continually adjusts, the corresponding voltage output is linear to the pressure (Figure 13). Because the microelectrode tips can fit inside compartments as small as a cell, measurements can be carefully taken from even the smallest vasculature and often without inflicting considerable damage.

The servo-null micropressure technique has been used to measure vascular pressure in developing chick embryos as well as for embryos surgically manipulated to induce disturbed hemodynamics.[65,129] Previous studies measured pressure with respect to disturbed mechanical loading within an individual aortic arch (AA), due to distortion of the OFT angle and growth of AA IV[130,131] to illustrate how alteration of wall stress, pressure and hemodynamic forces result in changes indicative of CHD.[132] Recently, Celik et al, simultaneously measured AA diameter using OCT guided technique while also measuring BP using the servo-null system in HH24 chick embryos[133] (Figure 14). Further, Sharma et al., measured simultaneous dorsal aortic BP and dorsal aortic blood velocity with a servo-null instrument (model 900A, WPI) mounted near the sinus venous, while imaging the dorsal aortic diameter.[134] Nakazawa et al.,[135] Clark et al.,[136,137] and Lucitti et al.[67] measured the arterial BP of chick embryos at different incubation days using the servo-null micropressure device. Nakazawa et al. in their study observed that heart rate, mean vitelline artery pressure, and mean dorsal aortic pressure shown in Figure 15 to increase with increased incubation time and temperature. In the meantime, Clark et al. investigated the effect of

	Stage	34.7° C	31.1° C	31.1° C	34.1° C
Heart rate (bpm)	18	151 ± 6	108 ± 5	107 ± 4	126 ± 3
	21	154 ± 4	111 ± 3	109 ± 6	134 ± 5
	24	169 ± 3	126 ± 3	127 ± 3	146 ± 3
Mean vitelline artery pressure (mm Hg)	18	0.69 ± 0.05	0.60 ± 0.05	0.52 ± 0.04	0.75 ± 0.06
	21	0.82 ± 0.03	0.72 ± 0.03	0.66 ± 0.05	0.87 ± 0.06
	24	1.05 ± 0.04	0.86 ± 0.07	0.93 ± 0.04	1.24 ± 0.06
Mean dorsal aortic blood flow (mm^3/s)	18	0.32 ± 0.02	0.21 ± 0.02	0.24 ± 0.02	0.31 ± 0.01
	21	0.49 ± 0.02	0.33 ± 0.02	0.34 ± 0.02	0.47 ± 0.02
	24	0.74 ± 0.04	0.43 ± 0.03	0.53 ± 0.04	0.74 ± 0.04
Vascular resistance (mm Hg/mm^3/s) ($\bar{x}$ ± 95% confidence interval)	18	2.18 ± 0.43	3.00 ± 0.86	2.22 ± 0.53	2.44 ± 0.53
	21	1.68 ± 0.19	2.23 ± 0.39	1.98 ± 0.42	1.86 ± 0.32
	24	1.44 ± 0.23	2.04 ± 0.45	1.81 ± 0.37	1.71 ± 0.30

FIGURE 15 Heart rate, mean vitelline artery pressure, mean dorsal aortic blood flow, and vascular resistance measurement at each environmental temperature. *Source*: replicated from Nakazawa et al.[135] with permission.

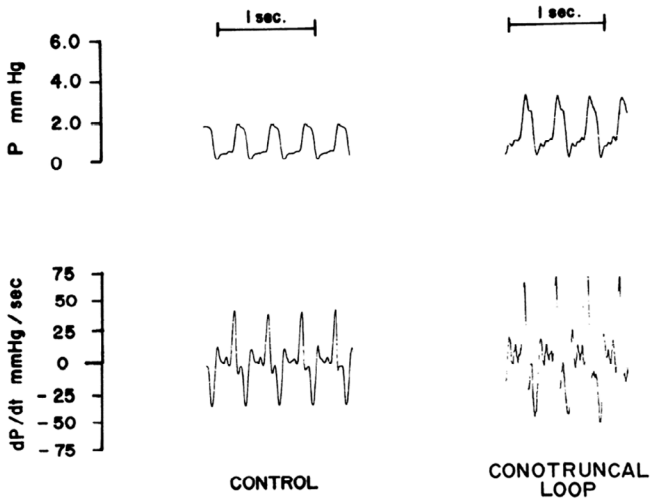

FIGURE 16 Measured ventricular phasic pressure and rate of pressure development (dP/dt). *Source*: replicated from Clark et al.[137] with permission.

arterial pressure on ventricular function and growth by using microsurgical ligation techniques, which acutely alter the arterial flow or arterial resistance (Figure 16).[137] Overall, both direct and indirect techniques to measure BP in embryos built a foundation on the development of BP in the chick embryo (Table 2).

2.3 | Measurement of BP in chick embryo using different techniques

The abovementioned techniques have been utilized to measure BP for developing chick embryos. The below table summarizes, the BP changes (HH18 to 27) during development that were measured with direct and indirect methods.

3 | SUMMARY AND OUTLOOK

The embryonic chick is a powerful animal model to study hemodynamic (blood flow, pressure) and developmental physiological changes during cardiac development and morphogenesis. Experimental induction of developmental cardiac defects, inducing hemodynamic alterations for embryonic chick can be achieved either surgically or chemically. These interventions predictably alter BP and flow velocities which can be measured via several complimentary methods. Most used applications for the chick embryo include Doppler Echocardiography and Doppler OCT for blood flow and catheter and servo null based systems for pressure measurements. While traditional techniques are beneficial, new approaches for cardiac physiology monitoring will advance chick embryo investigations significantly. For example, flow MRI has been shown to be very powerful in lager animal models such as mice but has not been utilized very commonly in the chick embryo due to the still high cost of MRI and related equipment. On the other hand, current pressure measurement systems such as catheter-based and servo-null micropressure systems are complicated and comparably invasive, and PIV systems are hindered by processing power. Hence there is a lot of room for improvement in physiological research in small, alternative (non-mammalian) model organisms. Conventional techniques have advantages and disadvantages, and proper technique needs to be selected for the specific application. Here we posit that modification of existing technologies has led to a considerable toolkit for investigating the hemodynamic development of the cardiovascular system in chicken embryos. The authors fully expect additional technologies to be applied to accommodate high throughput analysis of physiological phenotypes in experimental systems.

TABLE 2 Mean arterial pressure investigation during the embryonic developmental stages of chick using direct measurement (microcatheter), cannulation, and microscopic techniques.

References	Stage	Technique	Measurement location	Pressure (mmHg)	Condition
Girard[39]	HH18	Microcatheterization	Vitelline artery	0.52	Normal
Van Mierop and Bertuch[41]	HH20	Cannulation	Cardiac ventricles	0.91	Normal
Clark and Hu[7]	HH20	Direct puncture	Ventricles	1.02	Normal
	HH26	Direct puncture	Ventricles	2.35	Normal
Cheanvechai et al.[138]	HH24	Directly inserted	Ventricles	5.02	Normal
Rennie et al.[64]	HH18	Direct	Ventricles, aortic sac and dorsal aorta	0.80	Normal
Shi et al.[139]	HH18	Direct	Vitelline artery	0.82	Normal
	HH24	Direct	Vitelline artery	1.29	Normal
	HH27	Direct	Vitelline artery	1.26	Normal
McQuinn et al.[57]	HH24	Vevo 660 ultrasound bio microscope (55 MHz) and RM708 Scanhead	Outflow tract	0.98	Normal
Stekelenburg-de Vos et al.[121]	HH24-HH24	Stereomicroscopy and 900A	Vitelline vein	0.82	Normal
			Vitelline vein	1.15	Clipped
Shi et al.[139]	HH18	Directly inserted	Ventricle	0.65	OFT banded

Abbreviations: HH, Hamburger & Hamilton; OFT, outflow tract.

AUTHOR CONTRIBUTIONS

Vijayakumar Sukumaran: Investigation (equal); writing – original draft (equal). **Onur Mutlu:** Investigation (equal); writing – original draft (equal). **Mohammad Murtaza:** Writing – review and editing (equal). **Rawia Alhalbouni:** Writing – original draft (equal). **Benjamin Dubansky:** Writing – original draft (equal); writing – review and editing (equal).

FUNDING INFORMATION

This work was funded by Qatar National Research Fund (QNRF) and National Priority Research Program (Grant No. NPRP 10-0123-170222). Open Access funding was provided by the Qatar National Library.

ORCID

Vijayakumar Sukumaran https://orcid.org/0000-0002-2686-7329
Mohammad Murtaza https://orcid.org/0000-0002-5944-4963
Huseyin C. Yalcin https://orcid.org/0000-0003-3825-9934

REFERENCES

1. Angell SY, McConnell MV, Anderson CAM, et al. The American Heart Association 2030 impact goal: a presidential advisory from the American Heart Association. *Circulation*. 2020;141(9):e120-e138. doi:10.1161/CIR.0000000000000758
2. Liu Y, Chen S, Zühlke L, et al. Global birth prevalence of congenital heart defects 1970–2017: updated systematic review and meta-analysis of 260 studies. *Int J Epidemiol*. 2019;48(2):455-463. doi:10.1093/ije/dyz009
3. Boselli F, Freund JB, Vermot J. Blood flow mechanics in cardiovascular development. *Cell Mol Life Sci*. 2015;72(13):2545-2559. doi:10.1007/s00018-015-1885-3
4. Reckova M, Rosengarten C, de Almeida A, et al. Hemodynamics is a key epigenetic factor in development of the cardiac conduction system. *Circ Res*. 2003;93(1):77-85. doi:10.1161/01.RES.0000079488.91342.B7
5. Poelmann RE, Gittenberger-de Groot AC. Hemodynamics in cardiac development. *J Cardiovasc Dev Disease*. 2018;5(4):54. doi:10.3390/jcdd5040054
6. Lindsey SE, Butcher JT, Yalcin HC. Mechanical regulation of cardiac development. *Front Physiol*. 2014;5:318. doi:10.3389/fphys.2014.00318
7. Clark EB, Hu N. Developmental hemodynamic changes in the chick embryo from stage 18 to 27. *Circ Res*. 1982;51(6):810-815.
8. Davies PF. Hemodynamic shear stress and the endothelium in cardiovascular pathophysiology. *Nat Clin Pract Cardiovasc Med*. 2009;6(1):16-26. doi:10.1038/ncpcardio1397
9. Midgett M, Thornburg K, Rugonyi S. Blood flow patterns underlie developmental heart defects. *Am J Physiol Heart Circ Physiol*. 2017;312(3):H632-H642. doi:10.1152/ajpheart.00641.2016
10. Salman HE, Kamal RY, Yalcin HC. Numerical investigation of the fetal left heart hemodynamics during gestational stages. *Front Physiol*. 2021;12:731428. doi:10.3389/fphys.2021.731428

11. Salman HE, Kamal RY, Hijazi ZM, Yalcin HC. Hemodynamic and structural comparison of human fetal heart development between normally growing and hypoplastic left heart syndrome-diagnosed hearts. *Front Physiol*. 2022;13:856879. doi:10.3389/fphys.2022.856879
12. Flores-Santin J, Burggren WW. Beyond the chicken: alternative avian models for developmental physiological research. *Front Physiol*. 2021;12:712633. doi:10.3389/fphys.2021.712633
13. Bednarczyk M, Dunislawska A, Stadnicka K, Grochowska E. Chicken embryo as a model in epigenetic research. *Poult Sci*. 2021;100(7):101164. doi:10.1016/j.psj.2021.101164
14. Ruijtenbeek K, Mey JGRD, Blanco CE. The chicken embryo in developmental physiology of the cardiovascular system: a traditional model with new possibilities. *Am J Physiol Regul Integr Comp Physiol*. 2002;283(2):R549-R551. doi:10.1152/ajpregu.00107.2002
15. Alser M, Salman HE, Naija A, Seers TD, Khan T, Yalcin HC. Blood flow disturbance and morphological alterations following the right atrial ligation in the Chick embryo. *Front Physiol*. 2022;13:849603. doi:10.3389/fphys.2022.849603
16. Alser M, Shurbaji S, Yalcin HC. Mechanosensitive pathways in heart development: findings from Chick embryo studies. *J Cardiovasc Dev Dis*. 2021;8(4):32. doi:10.3390/jcdd8040032
17. Yalcin HC, Shekhar A, Nishimura N, Schaffer CB, Butcher JT. Abstract 19575: non-invasive creation of localized embryonic heart defects via multiphoton-guided femtosecond-laser photoablation. *Circulation*. 2010;122(suppl_21):A19575. doi:10.1161/circ.122.suppl_21.A19575
18. Dvorak HF. Angiogenesis: update 2005. *J Thromb Haemost*. 2005;3(8):1835-1842. doi:10.1111/j.1538-7836.2005.01361.x
19. Khurana R, Simons M, Martin JF, Zachary IC. Role of angiogenesis in cardiovascular disease: a critical appraisal. *Circulation*. 2005;112(12):1813-1824. doi:10.1161/CIRCULATIONAHA.105.535294
20. Baskurt OK, Meiselman HJ. Blood rheology and hemodynamics. *Semin Thromb Hemost*. 2003;29(5):435-450. doi:10.1055/s-2003-44551
21. Clark EB. Mechanisms in the pathogenesis of congenital cardiac malformations. In: Pierpont MEM, Moller JH, eds. *The Genetics of Cardiovascular Disease*. Boston, MA: Springer US; 1987:3-11.
22. Rose V, Clark E. Etiology of congenital heart disease. In: Freedom RM, Benson LN, Smallhorn JF, eds. *Neonatal Heart Disease*. London: Springer London; 1992:3-17.
23. Nora JJ. Etiologic factors in congenital heart diseases. *Pediat Clin N Am*. 1971;18(4):1059-1074. doi:10.1016/S0031-3955(16)32629-3
24. Peskin CS, Tu C. Hemodynamics in congenital heart disease. *Comput Biol Med*. 1986;16(5):331-359. doi:10.1016/0010-4825
25. Vanderlaan RD, Caldarone CA, Backx PH. Heart failure in congenital heart disease: the role of genes and hemodynamics. *Pflugers Arch*. 2014;466(6):1025-1035. doi:10.1007/s00424-014-1447-9
26. Lock JE. Hemodynamic evaluation of congenital heart disease. In: Lock JE, Keane JF, Fellows KE, eds. *Diagnostic and Interventional Catheterization in Congenital Heart Disease*. Boston, MA: Springer US; 1987:33-62.
27. Lutin WA, Brumund MR, Jones C, Tharpe CE, Montegomery M, McCaffrey FM. Hemodynamic abnormalities in fetuses with congenital heart disease. *Pediatr cardiol*. 1999;20(6):390-395. doi:10.1007/s002469900497
28. Foster FS, Zhang M, Duckett AS, Cucevic V, Pavlin CJ. In vivo imaging of embryonic development in the mouse eye by ultrasound biomicroscopy. *Invest Ophthalmol Vis Sci*. 2003;44(6):2361-2366. doi:10.1167/iovs.02-0911
29. Spencer KT, Kimura BJ, Korcarz CE, Pellikka PA, Rahko PS, Siegel RJ. Focused cardiac ultrasound: recommendations from the American Society of Echocardiography. *J Am Soc Echocardiogr*. 2013;26(6):567-581. doi:10.1016/j.echo.2013.04.001
30. Benslimane FM, Alser M, Zakaria ZZ, Sharma A, Abdelrahman HA, Yalcin HC. Adaptation of a mice doppler echocardiography platform to measure cardiac flow velocities for embryonic chicken and adult zebrafish [methods]. *Front Bioeng Biotechnol*. 2019;7:96. doi:10.3389/fbioe.2019.00096
31. Yelbuz TM, Choma MA, Thrane L, Kirby ML, Izatt JA. Optical coherence tomography: a new high-resolution imaging technology to study cardiac development in chick embryos. *Circulation*. 2002;106(22):2771-2774. doi:10.1161/01.cir.0000042672.51054.7b
32. Luo W, Marks DL, Ralston TS, Boppart SA. Three-dimensional optical coherence tomography of the embryonic murine cardiovascular system. *J Biomed Opt*. 2006;11(2):021014. doi:10.1117/1.2193465
33. Männer J, Thrane L, Norozi K, Yelbuz TM. High-resolution in vivo imaging of the cross-sectional deformations of contracting embryonic heart loops using optical coherence tomography. *Dev Dyn*. 2008;237(4):953-961. doi:10.1002/dvdy.21483
34. Karunamuni GH, Gu S, Ford MR, et al. Capturing structure and function in an embryonic heart with biophotonic tools. *Front Physiol*. 2014;5:351. doi:10.3389/fphys.2014.00351
35. Zurauskas M, Bradu A, Ferguson DR, Hammer DX, Podoleanu A. Closed loop tracked doppler optical coherence tomography based heart monitor for the Drosophila melanogaster larvae. *J Biophotonics*. 2016;9(3):246-252. doi:10.1002/jbio.201500007
36. Davis A, Izatt J, Rothenberg F. Quantitative measurement of blood flow dynamics in embryonic vasculature using spectral doppler velocimetry. *Anat Rec (Hoboken)*. 2009;292(3):311-319. doi:10.1002/ar.20808
37. Larina IV, Sudheendran N, Ghosn M, et al. Live imaging of blood flow in mammalian embryos using doppler swept-source optical coherence tomography. *J Biomed Opt*. 2008;13(6):060506. doi:10.1117/1.3046716
38. Yazdanfar S, Kulkarni M, Izatt J. High resolution imaging of in vivo cardiac dynamics using color doppler optical coherence tomography. *Opt Express*. 1997;1(13):424-431. doi:10.1364/oe.1.000424
39. Girard H. Arterial pressure in the chick embryo. *Am J Physiol*. 1973;224(2):454-460. doi:10.1152/ajplegacy.1973.224.2.454
40. Girard H. Adrenergic sensitivity of circulation in the chick embryo. *Am J Physiol*. 1973;224(2):461-469. doi:10.1152/ajplegacy.1973.224.2.461
41. Van Mierop LH, Bertuch CJ Jr. Development of arterial blood pressure in the chick embryo. *Am J Physiol*. 1967;212(1):43-48. doi:10.1152/ajplegacy.1967.212.1.43
42. Altimiras J, Dane A, Crossley I. Control of blood pressure mediated by baroreflex changes of heart rate in the chicken

embryo (Gallus gallus). *Am J Physiol Regul Integr Comp Physiol*. 2000;278(4):R980-R986. doi:10.1152/ajpregu.2000.278.4.R980
43. Hu N, Yost HJ, Clark EB. Cardiac morphology and blood pressure in the adult zebrafish. *Anat Rec*. 2001;264(1):1-12.
44. Sao K, Jones TM, Doyle AD, et al. Myosin II governs intracellular pressure and traction by distinct tropomyosin-dependent mechanisms. *Mol Biol Cell*. 2019;30(10):1170-1181. doi:10.1091/mbc.E18-06-0355
45. Holman E. Thoughts on the dynamics of blood flow. *Angiology*. 1950;1(6):530-533. doi:10.1177/000331975000100609
46. Hall JE. *Guyton and Hall Textbook of Medical Physiology E-Book*. Philadelphia, PA: Elsevier Health Sciences; 2015.
47. DeGroff CG. Doppler echocardiography. *Pediatr Cardiol*. 2002;23(3):307-333. doi:10.1007/s00246-001-0196-7
48. Hu N, Clark EB. Hemodynamics of the stage 12 to stage 29 chick embryo. *Circ Res*. 1989;65(6):1665-1670. doi:10.1161/01.RES.65.6.1665
49. Nakazawa M, Kajio F, Ikeda K, Takao A. Effect of atrial natriuretic peptide on hemodynamics of the stage 21 Chick embryo. *Pediatr Res*. 1990;27(6):557-560. doi:10.1203/00006450-199006000-00003
50. Huhta JC, Borges A, Yoon GY, Murdison KA, Wood DC. Noninvasive ultrasonic assessment of Chick embryo cardiac function. *Ann N Y Acad Sci*. 1990;588(1):383-386. doi:10.1111/j.1749-6632.1990.tb13240.x
51. Kowalski WJ, Pekkan K, Tinney JP, Keller BB. Investigating developmental cardiovascular biomechanics and the origins of congenital heart defects. *Front Physiol*. 2014;5:408. doi:10.3389/fphys.2014.00408
52. Yalcin HC, Shekhar A, McQuinn TC, Butcher JT. Hemodynamic patterning of the avian atrioventricular valve. *Dev Dyn*. 2011;240(1):23-35. doi:10.1002/dvdy.22512
53. Bharadwaj KN, Spitz C, Shekhar A, Yalcin HC, Butcher JT. Computational fluid dynamics of developing avian outflow tract heart valves. *Ann Biomed Eng*. 2012;40(10):2212-2227. doi:10.1007/s10439-012-0574-8
54. Quiñones MA, Otto CM, Stoddard M, Waggoner A, Zoghbi WA. Recommendations for quantification of doppler echocardiography: a report from the doppler quantification task force of the nomenclature and standards committee of the American Society of Echocardiography. *J Am Soc Echocardiogr*. 2002;15(2):167-184. doi:10.1067/mje.2002.120202
55. Keller BB, Kowalski WJ, Tinney JP, Tobita K, Hu N. Validating the paradigm that biomechanical forces regulate embryonic cardiovascular morphogenesis and are fundamental in the etiology of congenital heart disease. *J Cardiovasc Dev Disease*. 2020;7(2):23.
56. Anavekar NS, Oh JK. Doppler echocardiography: a contemporary review. *J Cardiol*. 2009;54(3):347-358. doi:10.1016/j.jjcc.2009.10.001
57. McQuinn TC, Bratoeva M, Dealmeida A, Remond M, Thompson RP, Sedmera D. High-frequency ultrasonographic imaging of avian cardiovascular development. *Dev Dyn*. 2007;236(12):3503-3513. doi:10.1002/dvdy.21357
58. Broekhuizen MLA, Mast F, Struijk PC, et al. Hemodynamic parameters of stage 20 to Stage 35 Chick embryo. *Pediatr Res*. 1993;34(1):44-46. doi:10.1203/00006450-199307000-00011
59. Phoon CKL. Imaging tools for the developmental biologist: ultrasound biomicroscopy of mouse embryonic development. *Pediatr Res*. 2006;60(1):14-21. doi:10.1203/01.pdr.0000219441.28206.79
60. Oosterbaan AM, Ursem NTC, Struijk PC, Bosch JG, van der Steen AFW, Steegers EAP. Doppler flow velocity waveforms in the embryonic chicken heart at developmental stages corresponding to 5–8 weeks of human gestation. *Ultrasound Obstet Gynecol*. 2009;33(6):638-644. doi:10.1002/uog.6362
61. Butcher JT, McQuinn TC, Sedmera D, Turner D, Markwald RR. Transitions in early embryonic atrioventricular valvular function correspond with changes in cushion biomechanics that are predictable by tissue composition. *Circ Res*. 2007;100(10):1503-1511. doi:10.1161/circresaha.107.148684
62. Salman HE, Alser M, Shekhar A, et al. Effect of left atrial ligation-driven altered inflow hemodynamics on embryonic heart development: clues for prenatal progression of hypoplastic left heart syndrome. *Biomech Model Mechanobiol*. 2021;20(2):733-750. doi:10.1007/s10237-020-01413-5
63. Hogers B, DeRuiter MC, ACG-D G, Poelmann RE. Unilateral vitelline vein ligation alters intracardiac blood flow patterns and morphogenesis in the Chick embryo. *Circ Res*. 1997;80(4):473-481. doi:10.1161/01.RES.80.4.473
64. Rennie MY, Stovall S, Carson JP, Danilchik M, Thornburg KL, Rugonyi S. Hemodynamics modify collagen deposition in the early embryonic chicken heart outflow tract. *J Cardiovasc Dev Disease*. 2017;4(4):24.
65. Midgett M, Rugonyi S. Congenital heart malformations induced by hemodynamic altering surgical interventions. *Front Physiol*. 2014;5:287. doi:10.3389/fphys.2014.00287
66. Hove JR, Koster RW, Forouhar AS, Acevedo-Bolton G, Fraser SE, Gharib M. Intracardiac fluid forces are an essential epigenetic factor for embryonic cardiogenesis. *Nature*. 2003;421(6919):172-177. doi:10.1038/nature01282
67. Lucitti JL, Tobita K, Keller BB. Arterial hemodynamics and mechanical properties after circulatory intervention in the chick embryo. *J Exp Biol*. 2005;208(10):1877-1885. doi:10.1242/jeb.01574
68. Pang KL, Parnall M, Loughna S. Effect of altered haemodynamics on the developing mitral valve in chick embryonic heart. *J Mol Cell Cardiol*. 2017;108:114-126. doi:10.1016/j.yjmcc.2017.05.012
69. Hogers B, DeRuiter MC, Gittenberger-de Groot AC, Poelmann RE. Extraembryonic venous obstructions lead to cardiovascular malformations and can be embryolethal. *Cardiovasc Res*. 1999;41(1):87-99. doi:10.1016/s0008-6363
70. Salman HE, Yalcin HC. Advanced blood flow assessment in zebrafish via experimental digital particle image velocimetry and computational fluid dynamics modeling. *Micron*. 2020;130:102801. doi:10.1016/j.micron.2019.102801
71. Huang D, Swanson EA, Lin CP, et al. Optical coherence tomography. *Science*. 1991;254(5035):1178-1181. doi:10.1126/science.1957169
72. Yonetsu T, Bouma BE, Kato K, Fujimoto JG, Jang IK. Optical coherence tomography- 15 years in cardiology. *Circ J*. 2013;77(8):1933-1940. doi:10.1253/circj.cj-13-0643.1
73. Lansford R, Rugonyi S. Follow me! A tale of avian heart development with comparisons to mammal heart development. *J Cardiovasc Dev Disease*. 2020;7(1):8.
74. Daqing P, Nan Guang C, Quing Z, Dutta NK, Otis LL. *Imaging of fluid flow velocity using doppler optical coherence*

tomography: preliminary results. Proceedings of the IEEE 27th Annual Northeast Bioengineering Conference (Cat. No.01CH37201), IEEE, 2001. p. 55–56.
75. Huber R, Adler DC, Fujimoto JG. Buffered Fourier domain mode locking: unidirectional swept laser sources for optical coherence tomography imaging at 370,000 lines/s. *Opt Lett*. 2006;31(20):2975-2977. doi:10.1364/OL.31.002975
76. Choma MA, Sarunic MV, Yang C, Izatt JA. Sensitivity advantage of swept source and Fourier domain optical coherence tomography. *Opt Express*. 2003;11(18):2183-2189. doi:10.1364/OE.11.002183
77. Jenkins MW, Rothenberg F, Roy D, et al. 4D embryonic cardiography using gated optical coherence tomography. *Opt Express*. 2006;14(2):736-748. doi:10.1364/OPEX.14.000736
78. Chen Z, Milner TE, Srinivas S, et al. Noninvasive imaging of in vivo blood flow velocity using optical doppler tomography. *Opt Lett*. 1997;22(14):1119-1121. doi:10.1364/ol.22.001119
79. Taber LA, Zhang J, Perucchio R. Computational model for the transition from peristaltic to pulsatile flow in the embryonic heart tube. *J Biomech Eng*. 2007;129(3):441-449. doi:10.1115/1.2721076
80. van Leeuwen TG, Kulkarni MD, Yazdanfar S, Rollins AM, Izatt JA. High-flow-velocity and shear-rate imaging by use of color doppler optical coherence tomography. *Opt Lett*. 1999;24(22):1584-1586. doi:10.1364/OL.24.001584
81. Rugonyi S, Shaut C, Liu A, Thornburg K, Wang RK. Changes in wall motion and blood flow in the outflow tract of chick embryonic hearts observed with optical coherence tomography after outflow tract banding and vitelline-vein ligation. *Phys Med Biol*. 2008;53(18):5077-5091. doi:10.1088/0031-9155/53/18/015
82. Ma Z, Liu A, Yin X, et al. Measurement of absolute blood flow velocity in outflow tract of HH18 chicken embryo based on 4D reconstruction using spectral domain optical coherence tomography. *Biomed Opt Express*. 2010;1(3):798-811. doi:10.1364/boe.1.000798
83. Lopez AL 3rd, Wang S, Larin KV, Overbeek PA, Larina IV. Live four-dimensional optical coherence tomography reveals embryonic cardiac phenotype in mouse mutant. *J Biomed Opt*. 2015;20(9):090501. doi:10.1117/1.JBO.20.9.090501
84. van Geuns RJ, Wielopolski PA, de Bruin HG, et al. Basic principles of magnetic resonance imaging. *Prog Cardiovasc Diseases*. 1999;42(2):149-156. doi:10.1016/s0033-0620(99)70014-9
85. Constantine G, Shan K, Flamm SD, Sivananthan MU. Role of MRI in clinical cardiology. *Lancet*. 2004;363(9427):2162-2171. doi:10.1016/s0140-6736(04)16509-4
86. Powell AJ, Geva T. Blood flow measurement by magnetic resonance imaging in congenital heart disease. *Pediatr Cardiol*. 2000;21(1):47-58. doi:10.1007/s002469910007
87. Mathew RC, Löffler AI, Salerno M. Role of cardiac magnetic resonance imaging in valvular heart disease: diagnosis, assessment, and management. *Curr Cardiol Rep*. 2018;20(11):119. doi:10.1007/s11886-018-1057-9
88. Cawley PJ, Maki JH, Otto CM. Cardiovascular magnetic resonance imaging for valvular heart disease: technique and validation. *Circulation*. 2009;119(3):468-478. doi:10.1161/circulationaha.107.742486
89. White JA, Patel MR. The role of cardiovascular MRI in heart failure and the cardiomyopathies. *Magn Reson Imaging Clin N Am*. 2007;15(4):541-564. doi:10.1016/j.mric.2007.08.009
90. Steel KE, Kwong RY. Application of cardiac magnetic resonance imaging in cardiomyopathy. *Curr Heart Fail Rep*. 2008;5(3):128-135. doi:10.1007/s11897-008-0021-1
91. Hartnell GG. Imaging of aortic aneurysms and dissection: CT and MRI. *J Thorac Imaging*. 2001;16(1):35-46. doi:10.1097/00005382-200101000-00006
92. Rajiah P. CT and MRI in the evaluation of thoracic aortic diseases. *J Vasc Med*. 2013;2013:1-16. doi:10.1155/2013/797189
93. Habets J, Zandvoort HJ, Reitsma JB, et al. Magnetic resonance imaging is more sensitive than computed tomography angiography for the detection of endoleaks after endovascular abdominal aortic aneurysm repair: a systematic review. *Eur J Vasc Endovasc Surg*. 2013;45(4):340-350. doi:10.1016/j.ejvs.2012.12.014
94. Shepherd B, Abbas A, McParland P, et al. MRI in adult patients with aortic coarctation: diagnosis and follow-up. *Clin Radiol*. 2015;70(4):433-445. doi:10.1016/j.crad.2014.12.005
95. Pepe A, Li J, Rolf-Pissarczyk M, et al. Detection, segmentation, simulation and visualization of aortic dissections: a review. *Med Image Anal*. 2020;65:101773. doi:10.1016/j.media.2020.101773
96. Bone SN, Johnson GA, Thompson MB. Three-dimensional magnetic resonance microscopy of the developing chick embryo. *Invest Radiol*. 1986;21(10):782-787. doi:10.1097/00004424-198610000-00003
97. Johnson GA, Thompson MB, Drayer BP, Bone SN. Magnetic resonance microscopy in neurologic models. *Acta Radiol Suppl*. 1986;369:267-268.
98. Smith BR, Johnson GA, Groman EV, Linney E. Magnetic resonance microscopy of mouse embryos. *Proc Natl Acad Sci U S A*. 1994;91(9):3530-3533. doi:10.1073/pnas.91.9.3530
99. Smith BR, Linney E, Huff DS, Johnson GA. Magnetic resonance microscopy of embryos. *Comput Med Imaging Graph*. 1996;20(6):483-490. doi:10.1016/S0895-6111(96)00046-8
100. Bain MM, Fagan AJ, Mullin JM, McNaught I, McLean J, Condon B. Noninvasive monitoring of chick development in ovo using a 7T MRI system from day 12 of incubation through to hatching. *J Magn Reson Imaging*. 2007;26(1):198-201. doi:10.1002/jmri.20963
101. Zhou Z, Chen Z, Shan J, et al. Monitoring brain development of chick embryos in vivo using 3.0 T MRI: subdivision volume change and preliminary structural quantification using DTI. *BMC Dev Biol*. 2015;15(1):29. doi:10.1186/s12861-015-0077-6
102. Goodall N, Kisiswa L, Prashar A, et al. 3-dimensional modelling of chick embryo eye development and growth using high resolution magnetic resonance imaging. *Exp Eye Res*. 2009;89(4):511-521. doi:10.1016/j.exer.2009.05.014
103. Parasoglou P, Berrios-Otero CA, Nieman BJ, Turnbull DH. High-resolution MRI of early-stage mouse embryos. *NMR Biomed*. 2013;26(2):224-231. doi:10.1002/nbm.2843
104. Norris FC, Siow BM, Cleary JO, et al. Diffusion microscopic MRI of the mouse embryo: protocol and practical implementation in the splotch mouse model. *Magn Reson Med*. 2015;73(2):731-739. doi:10.1002/mrm.25145
105. Berrios-Otero CA, Wadghiri YZ, Nieman BJ, Joyner AL, Turnbull DH. Three-dimensional micro-MRI analysis of

cerebral artery development in mouse embryos. *Magn Reson Med*. 2009;62(6):1431-1439. doi:10.1002/mrm.22113
106. Effmann EL, Johnson GA, Smith BR, Talbott GA, Cofer G. Magnetic resonance microscopy of chick embryos in ovo. *Teratology*. 1988;38(1):59-65. doi:10.1002/tera.1420380109
107. Smith BR, Effmann EL, Johnson GA. MR microscopy of chick embryo vasculature. *J Magn Reson Imaging*. 1992;2(2):237-240. doi:10.1002/jmri.1880020220
108. Holmes WM, McCabe C, Mullin JM, Condon B, Bain MM. Noninvasive self-gated magnetic resonance cardiac imaging of developing chick embryos in ovo. *Circulation*. 2008;117(21):e346-e347. doi:10.1161/CIRCULATIONAHA.107.747154
109. Herrmann A, Taylor A, Murray P, Poptani H, Sée V. Magnetic resonance imaging for characterization of a Chick embryo model of cancer cell metastases. *Mol Imaging*. 2018;17:1536012118809585. doi:10.1177/1536012118809585
110. Zuo Z, Syrovets T, Genze F, et al. High-resolution MRI analysis of breast cancer xenograft on the chick chorioallantoic membrane. *NMR Biomed*. 2015;28(4):440-447. doi:10.1002/nbm.3270
111. Duce S, Morrison F, Welten M, Baggott G, Tickle C. Micro-magnetic resonance imaging study of live quail embryos during embryonic development. *Magn Reson Imaging*. 2011;29(1):132-139. doi:10.1016/j.mri.2010.08.004
112. Eckrich J, Kugler P, Buhr CR, et al. Monitoring of tumor growth and vascularization with repetitive ultrasonography in the chicken chorioallantoic-membrane-assay. *Sci Rep*. 2020;10(1):18585. doi:10.1038/s41598-020-75660-y
113. Zou P, Li M, Wang Z, et al. Micro-particle image velocimetry investigation of flow fields of SonoVue microbubbles mediated by ultrasound and their relationship with delivery. *Front Pharmacol*. 2019;10:1651. doi:10.3389/fphar.2019.01651
114. Tho P, Manasseh R, Ooi A. Cavitation microstreaming patterns in single and multiple bubble systems. *J Fluid Mech*. 2007;576:191-233. doi:10.1017/S0022112006004393
115. Collis J, Manasseh R, Liovic P, et al. Cavitation microstreaming and stress fields created by microbubbles. *Ultrasonics*. 2010;50(2):273-279. doi:10.1016/j.ultras.2009.10.002
116. Chen C-Y, Menon PG, Kowalski W, Pekkan K. Time-resolved OCT-μPIV: a new microscopic PIV technique for noninvasive depth-resolved pulsatile flow profile acquisition. *Exp Fluids*. 2012;54(1):1426. doi:10.1007/s00348-012-1426-x
117. Yalcin HC. Femtosecond laser photodisruption of vitelline vessels of avian embryos as a technique to study embryonic vascular remodeling. *Exp Biol Med*. 2014;239(12):1644-1652. doi:10.1177/1535370214546272
118. Reuter F, Gonzalez-Avila SR, Mettin R, Ohl C-D. Flow fields and vortex dynamics of bubbles collapsing near a solid boundary. *Phys Rev Fluids*. 2017;2(6):064202. doi:10.1103/PhysRevFluids.2.064202
119. Yoshigi M, Hu N, Keller BB. Dorsal aortic impedance in stage 24 chick embryo following acute changes in circulating blood volume. *Am J Physiol*. 1996;270(5 Pt 2):H1597-H1606. doi:10.1152/ajpheart.1996.270.5.H1597
120. Sharma SK, Lucitti JL, Nordman C, Tinney JP, Tobita K, Keller BB. 12 impact of hypoxia on early Chick embryo growth and cardiovascular function. *Pediatr Res*. 2005;58(4):818. doi:10.1203/00006450-200510000-00042
121. Stekelenburg-de Vos S, Ursem N, Hop W, Wladimiroff J, Gittenberger-de Groot A, Poelmann R. Acutely altered hemodynamics following venous obstruction in the early chick embryo. *J Exp Biol*. 2003;206(6):1051-1057. doi:10.1242/jeb.00216
122. Dane A, Crossley I, Burggren WW, Altimiras J. Cardiovascular regulation during hypoxia in embryos of the domestic chicken Gallus gallus. *Am J Physiol Regul Integr Compar Physiol*. 2003;284(1):R219-R226. doi:10.1152/ajpregu.00654.2001
123. Diletti R, Van Mieghem NM, Valgimigli M, et al. Rapid exchange ultra-thin microcatheter using fibre-optic sensing technology for measurement of intracoronary fractional flow reserve. *EuroIntervention*. 2015;11(4):428-432. doi:10.4244/eijy15m05_09
124. Paff GH, Boucek RJ, Gutten GS. Ventricular blood pressures and competency of valves in the early embryonic chick heart. *Anat Rec*. 1965;151(2):119-123. doi:10.1002/ar.1091510203
125. Tazawa H. Measurement of blood pressure of chick embryo with an implanted needle catheter. *J Appl Physiol*. 1981;51(4):1023-1026. doi:10.1152/jappl.1981.51.4.1023
126. Tazawa H, Nakagawa S. Response of egg temperature, heart rate and blood pressure in the chick embryo to hypothermal stress. *J Comp Physiol B*. 1985;155(2):195-200. doi:10.1007/BF00685213
127. Grabowski CT, Tsai ENC, Toben HR. The effects of teratogenic doses of hypoxia on the blood pressure of chick embryos. *Teratology*. 1969;2(1):67-76. doi:10.1002/tera.1420020109
128. Rajala GM, Kaplan S. Abnormally elevated blood pressure in the trypan blue-treated chick embryo during early morphogenesis. *Teratology*. 1980;21(2):247-251. doi:10.1002/tera.1420210215
129. Midgett M, López CS, David L, Maloyan A, Rugonyi S. Increased hemodynamic load in early embryonic stages alters myofibril and mitochondrial Organization in the Myocardium [original research]. *Front Physiol*. 2017;2017:8. doi:10.3389/fphys.2017.00631
130. Kowalski WJ, Dur O, Wang Y, et al. Critical transitions in early embryonic aortic arch patterning and hemodynamics. *PLOS One*. 2013;8(3):e60271. doi:10.1371/journal.pone.0060271
131. Sedmera D, Pexieder T, Rychterova V, Hu N, Clark EB. Remodeling of chick embryonic ventricular myoarchitecture under experimentally changed loading conditions. *Anat Rec*. 1999;254(2):238-252. doi:10.1002/(sici)1097-0185(19990201)254:2<238::Aid-ar10>3.0.Co;2-v
132. Biechler SV, Junor L, Evans AN, et al. The impact of flow-induced forces on the morphogenesis of the outflow tract. *Front Physiol*. 2014;5:225. doi:10.3389/fphys.2014.00225
133. Celik M, Goktas S, Karakaya C, et al. Microstructure of early embryonic aortic arch and its reversibility following mechanically altered hemodynamic load release. *Am J Physiol Heart Circ Physiol*. 2020;318(5):H1208-h1218. doi:10.1152/ajpheart.00495.2019
134. Sharma SK, Lucitti JL, Nordman C, Tinney JP, Tobita K, Keller BB. Impact of hypoxia on early Chick embryo growth and cardiovascular function. *Pediatr Res*. 2006;59(1):116-120. doi:10.1203/01.pdr.0000191579.63339.90
135. Nakazawa M, Clark EB, Hu N, Wispé J. Effect of environmental hypothermia on vitelline artery blood pressure and

vascular resistance in the stage 18, 21, and 24 chick embryo. *Pediatr Res*. 1985;19(7):651-654. doi:10.1203/00006450-198507000-00003

136. Clark EB, Hu N, Dummett JL, Vandekieft GK, Olson C, Tomanek R. Ventricular function and morphology in chick embryo from stages 18 to 29. *Am J Physiol*. 1986; 250(3 Pt 2):H407-H413. doi:10.1152/ajpheart.1986.250.3.H407
137. Clark EB, Hu N, Frommelt P, Vandekieft GK, Dummett JL, Tomanek RJ. Effect of increased pressure on ventricular growth in stage 21 chick embryos. *Am J Physiol*. 1989;257(1 Pt 2):H55-H61. doi:10.1152/ajpheart.1989.257.1.H55
138. Cheanvechai V, Hughes SF, Benson DW Jr. Relationship between cardiac cycle length and ventricular relaxation rate in the chick embryo. *Pediatr Res*. 1992;31(5):480-482. doi:10.1203/00006450-199205000-00014
139. Shi L, Goenezen S, Haller S, Hinds MT, Thornburg KL, Rugonyi S. Alterations in pulse wave propagation reflect the degree of outflow tract banding in HH18 chicken embryos. *Am J Physiol Heart Circ Physiol*. 2013;305(3):H386-H396. doi:10.1152/ajpheart.00100.2013

How to cite this article: Sukumaran V, Mutlu O, Murtaza M, Alhalbouni R, Dubansky B, Yalcin HC. Experimental assessment of cardiovascular physiology in the chick embryo. *Developmental Dynamics*. 2023;1-22. doi:10.1002/dvdy.589